Evaluation and Optimization of Axial Air Gap Propulsion Motors for Naval Vessels

by

Mark W. Thomas

B.S., Electrical Engineering (1984)
Oklahoma State University

Submitted to the Departments of Ocean Engineering and Electrical Engineering
in Partial Fulfillment of the Requirements for the Degrees of
NAVAL ENGINEER
and
MASTER of SCIENCE
in
ELECTRICAL ENGINEERING and COMPUTER SCIENCE
at the
MASSACHUSETTS INSTITUTE OF TECHNOLOGY
June 1996

Signature of Author: _____
Departments of Ocean Engineering and Electrical Engineering
May 6, 1996

Certified by: _____
James L. Kirtley Jr., Thesis Supervisor
Professor of Electrical Engineering

Certified by: _____
A. Douglas Carmichael, Thesis Reader
Professor of Power Engineering

Accepted by: _____
A. Douglas Carmichael, Chairman
Department of Ocean Engineering
Committee for Graduate Students

Accepted by: _____
F. R. Morgenthaler, Graduate Officer
Department of Electrical Engineering and Computer Science

Evaluation and Optimization of Axial Air Gap Propulsion Motors for Naval Vessels

by

Mark W. Thomas

Submitted to the Departments of Ocean and Electrical Engineering on May 10, 1996 in partial fulfillment of the requirements for the degrees of Naval Engineer and Master of Science in Electrical Engineering and Computer Science.

ABSTRACT

A unique method is used to optimize a design to multi-objective criteria. While the method is potentially applicable to any optimization where the cost function is not well defined, the products considered here are synchronous axial gap electric motors (both wound rotor and permanent magnet) and the application for which the motors are optimized is warship propulsion. All motors are rated at 40,000 hp, or approximately 25 megawatts.

A preliminary design of an axial gap motor in this power range was completed as part of doctoral research by T. J. McCoy [1]. All wound rotor designs in this study are based on his work. However, the McCoy motor includes a rotating thermosyphon cooling system, which is omitted here in favor of a simple heat density calculation. A permanent magnet machine design is presented and the resulting motors are optimized simultaneously with wound rotor types based on Naval propulsion criteria.

This optimization method was originated by J. A. Moses et al. [2] and is termed the Novice Design Assistant. It involves the repetitive computer generation of designs through random combinations of design parameters. The results are compared to a database of previous designs. Any design found to be dominated in all desired attributes by another is discarded; otherwise it is added to the database. Dominance is determined by an evaluator module, tailored to the application, which compares motor attributes such as physical dimensions, weight and efficiency. The result of many iterations is an n-dimensional "frontier" of non-dominated designs, where n is the number of attributes considered. Since the number of feasible possibilities is large given that some design parameters may vary continuously, a low "hit" rate is avoided by mapping successful parameter combinations back to the design module using a Gaussian distribution. This mapping process is similar to that used by U. Sinha in applying the method to commercial induction motors [3], and preserves the creativity of the method while decreasing computer overhead time.

Thesis supervisor: James L. Kirtley Jr.
Title: Professor of Electrical Engineering

Biographical Note

The author graduated from Oklahoma State University in May of 1984 with a Bachelor of Science degree in Electrical Engineering. He attended the Navy's Officer Candidate School in Newport, Rhode Island and was commissioned as an Ensign in the US Navy in October 1984. He served as a division officer aboard the destroyer USS David R. Ray (DD-971) for four years, qualifying as a Surface Warfare Officer and Gas Turbine Engineering Officer of the Watch. Further tours included instructor duty at Gas Turbine Engineering Officer of the Watch School in San Diego and two years as a main propulsion inspector at the Pacific Board of Inspection and Survey, after joining the Navy's Engineering Duty Officer community. He reported to MIT in June of 1993 for a three year tour of full time graduate work in the Naval Architecture and Marine Engineering (13A) program of the Ocean Engineering department.

Table of Contents

List of Figures

1. Introduction

1.1 Electric Propulsion of Naval Vessels

Electric motor propulsion of Navy warships has been of interest to naval architects through several generations of ships, but has not been widely implemented despite the fact that its potential benefits are significant. Electric propulsion allows nearly complete elimination of the propulsion shaft and its considerable weight and space requirements, resulting in a higher payload fraction or increased endurance. Design flexibility is greatly enhanced, as the machinery arrangement is not constrained by the shaft. Prime mover efficiency, lifetime, and maintainability are increased because of the inherent cross-connecting capability. Main reduction gears, with their associated weight, volume and high replacement costs, are eliminated. Also, electric propulsion lends itself well to an "integrated ship" concept where all electrical loads, propulsion and non-propulsion, are fed from a common bus powered by identical prime movers. The distinction between the electrical and the propulsion systems is thus removed, the ship is less complex and more robust, and energy is utilized more efficiently.

Several obstacles, both technical and non-technical, have prevented broad implementation of electric propulsion in the past. Apart from the common perceptions of increased cost and risk, perhaps the most prominent obstacle has been motor cooling. This is a result of the high power densities required due to space constraints aboard ship. If a motor is made large enough to allow air or water cooling, it may exceed the arrangeable area available and its radius may cause an unsatisfactory shaft angle. Shaft angles greater than five or six degrees from horizontal result in degraded efficiency due to the downward component of propeller thrust. Some conceptual electric propulsion systems using large motors have required direction changing gears between the motor and propeller for this reason, adding weight and negating some of the benefit of the systems.

Several options have been proposed to overcome cooling and arrangement difficulties in implementing electric drive. These include the utilization of super-conducting field windings, which allow for larger internal shear forces per rotor volume but do not reduce the amount of back iron required to carry the flux densities. Overall size reductions have been realized; however, this type of technology also increases the complexity of the motor and requires secondary support systems of its own, such as cryogenic cooling and dedicated storage and analysis facilities. Acyclic machines, another possible solution, are also capable of producing relatively intense fields but are burdened with the same requirement for back iron and possibly cryogenics and liquid metal contacts. One of the latest subjects of research has been advanced permanent magnet motors, which also are capable of producing large power densities and high efficiencies, but likewise do not solve the problems of saturation and cooling.

The options considered to date have focused primarily on improvements to motors with radially directed flux. It can be shown using purely geometric arguments that if flux is directed axially by using stacked disks for the rotor and stator that the required volume per unit torque decreases. This is obviously beneficial where space is constrained, as in warship propulsion. Also, it is possible to place several rotor and stator disk pairs on the same shaft resulting in a longer rather than a wider motor for increased power. This helps to remedy the shaft angle problem discussed above. Figure 1-1 shows simplified drawings of the two motor types and their flux paths.

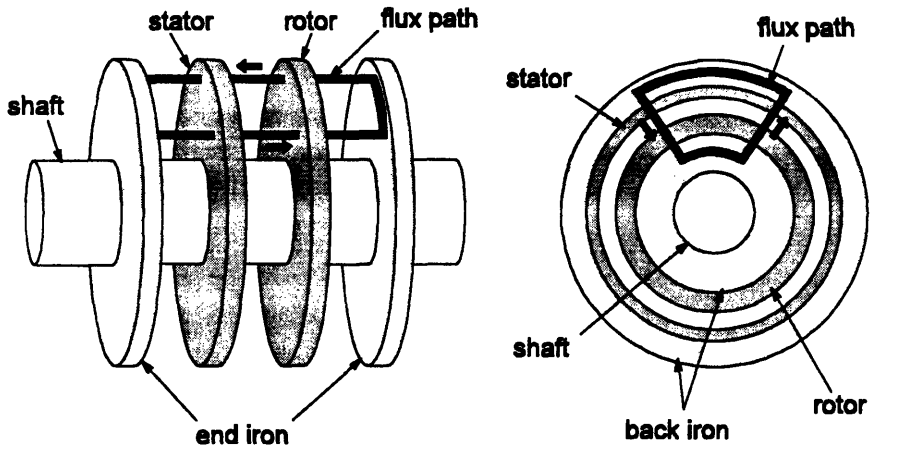

Figure 1-1: Electric Motor Flux Paths

At the time of this writing, no particular motor type has been designated as the most promising for implementing electric propulsion in Navy ships, although it is relatively certain that some 21st century warships will be electrically propelled [4]. The axial flux (or axial gap) motor is a promising technology and its preliminary design must be optimized in order to perform meaningful cost-benefit analyses for these future ships. The objective of this study is that optimization.

1.2 Multi-objective Optimization

In a certain sense, design is a problem in optimization. Rather than attempting to formulate a product that simply satisfies requirements, a designer is generally interested in optimizing design features to result in the "best" product possible. Of course, there are always unlimited design possibilities that are not physically feasible or do not satisfy requirements (such as power rating), but there are also potentially unlimited possibilities that do. In order to select a manageably sized set of acceptable designs for further evaluation, some method of ranking feasible possibilities in terms of their relative usefulness must be employed. Usefulness is, at least in part, a function of the product's intended application and depends on the product's characteristics, or *attributes*. Attributes may include the product's efficiency, weight, size, cost, expected lifetime, etc.

and make up the set of characteristics that are of interest to the customer, given that the product meets basic requirements.

There are numerous proven methods for optimizing a given mathematical function. Regardless of the number of variables involved, the goal is to determine the location of the function's maxima (or equivalently the minima of the complementary function). The function to be optimized is commonly known as the "cost" function. It does not indicate actual monetary cost, although monetary cost may be a dependent variable. The methods available for optimization of cost functions vary in terms of their accuracy, the number of iterations required for convergence and the complexity of the calculations involved. The preferred method of optimization and its measure of success are largely determined by the function itself in terms of its linearity, continuity, relative magnitudes of gradients, local and global positive definiteness, etc. Usually one or more methods are adequate in terms of accuracy and required processing time to locate maxima of a given function.

In design optimization, however, a unique cost function generally does not exist. For example, if one is to design a motor for ship propulsion, one would normally strive for high efficiency, low volume, low weight and good reliability, among other characteristics. However, there is no mathematical function available for determining which combination of these attributes results in the most useful motor. Obviously high efficiency is desirable, but whether an additional percentage point of efficiency is worth, for example, a given increase in the machine's acquisition cost is undetermined without unusually detailed and informed customer specifications.

Numerous methods have been proposed for overcoming this situation; many of them are variations of what is commonly known as a decision matrix, or decision tree. This method is based on relative *subjective* weighting of the attributes. For example, a customer (or designer) might come to the conclusion through experience, intuition or executive guidance that motor efficiency is twice as important as cost. Then a given percentage increase in efficiency would be "worth" up to twice this percentage increase in cost. If a pair-wise weighting scheme such as this is carried out for all attributes, motors can be "scored" based on their attributes and the designer can attempt to maximize this score by variation of design parameters. If the weightings are formalized in a spreadsheet or computer program, the evaluation can be automated and the final score of a design becomes its only relevant characteristic. A procedure such as this may create some sense of objectivity, since designs are numerically ranked, when in fact its foundation is subjective. In the absence of a cost function, the decision tree method essentially creates one. The attribute weightings assigned are not absolutes and may vary with the individual or individuals assigning them; they may be inconsistent even when assigned by the same person at different times. Obviously it can be considered hazardous to make a selection based on such a method, particularly when considerable expenditures of time and money are involved and the decision is not easily reversed.

In the search for objectivity in such cases, one might be lead to consider the attributes to be *independent* and attempt to define their individual optimum values. Then the "best"

design would be the one that scores higher than all other designs in *all* attributes; this would eliminate the subjectivity involved in determining the relative importance of attributes. If this approach is taken, optimum values of some motor attributes mentioned above become self-evident. Obviously the "best" value of efficiency is 100%, the "best" weight is zero, etc. For others, the answer is not as simple and may be dependent upon the application. Physical dimensions are a good example of this. As mentioned before, motors with small radii are desirable in Navy propulsion due to shaft angle considerations. However, if decreased radius results in increased length, then the number of supporting bearings or the shaft radius must also increase, raising acquisition cost, maintenance requirements and possibly machine weight. Also, as the motor becomes longer, it may eventually exceed the length of the space in which it is to be installed. Considerations such as this show that even if attributes are considered independent, some subjective judgment may be unavoidable in assigning their individual optimum values. The subjectivity is much more limited, however, than in the pair-wise comparison method previously discussed.

Assuming that individual attribute optima can be assigned, it is possible to eliminate many feasible designs from consideration simply because they are inferior in *all* respects to some other design. Such inferior but feasible designs are said to be dominated. This is the essence of the Novice Design method used in this study. The set remaining after all dominated designs have been discarded will comprise an n-dimensional frontier of non-dominated designs, where n is the number of attributes evaluated. Note that no conclusions may be drawn regarding the relative usefulness of the non-dominated designs, because no weightings are assigned to the attributes during evaluation. However, the size of the solution set will have been reduced and those that comprise it will be *more* appropriate for the application than any of those eliminated. Employing such a procedure to eliminate inferior designs from consideration may also give some insight into the parameter values that tend to result in the best designs. For example, if a certain parameter is present only in a small range of values for all non-dominated designs, one might be lead to restrict the range of this parameter in future analyses. This would reduce design time while avoiding the possibility of neglecting unforeseen but useful combinations.

Obviously, a method such as this requires a pre-existing set of designs and the results obtainable are dependent on the number of designs considered. A large initial set of feasible designs is necessary, and this requirement naturally leads to computer generation. If the design process can be reduced to combining parameters in a random or pseudo-random fashion such that all combinations are guaranteed to satisfy minimum customer requirements, then the number of designs available for consideration is limited only by computer run time. If each design output is sent to an attribute evaluator which objectively and individually compares its attributes with other designs based on pre-defined optimum values, it is then possible to automatically eliminate all dominated designs from the solution set and the result is the frontier mentioned above.

The method by which the design parameters are specified during each iteration will affect the ratio of dominated to non-dominated outputs; a non-dominated output is termed a "hit". The parameter specification process may be allowed to be totally random or may be influenced in some way in order to increase the hit rate. This influencing will normally involve some method of mapping successful parameter combinations back to the design module from the evaluator. In this study, the mapping method chosen is a Gaussian distribution, but many other methods are available such as sensitivity analyses and variations of the hill-climbing techniques used in mathematical optimization.

An optimization routine such as this is not the only application of the Novice method. For example, rather than specifying the customer requirements and forcing all designs to meet them, the designs may be generated randomly without regard to requirements, the only constraint being physical feasibility. The results may then be evaluated in terms of the requirements, retaining only those which satisfy them and discarding those which do not. This might be termed a pure design application, as opposed to the optimization application used here. A design application might be preferred if the programming of the designer to generate exclusively customer feasible designs was exceptionally complex, or if the intended use of the product was undefined or very general. The design application has been studied for commercial induction motors by Sinha [3].

2. Axial Gap Motor Design

The method chosen to produce the large set of feasible motors necessary for this study is random computer generation. This chapter begins with a discussion of the general nature of the design code developed and the design parameters selected for random variation. This is followed by a detailed analysis of the design process and the algorithms used. Physical constants and other resident variables in the code are listed in Appendix A; the MATLAB™ macro is contained in Appendix B.

2.1 Design Overview

Portions of the design code are based on the McCoy motor [1], although certain elements of his design are analyzed in greater detail and new algorithms are developed. These include edge turns, leakage flux, shaft stresses, off-rated efficiency and the radial dependence of flux density in the disk teeth. Other elements, such as the extensive heat transfer analysis in McCoy's work, are simplified or omitted when their effects do not impact the attribute comparison process. The radial heat pipes of the McCoy motor and the additional structure necessary to accommodate them are not modeled.

An elementary acquisition cost model is developed and used in conjunction with projected fuel usage to obtain a lifecycle cost figure. While care is taken to make this model as legitimate as possible, its purpose is to determine relative cost differences among the motors. It is not intended to be a precise estimator of any particular motor's actual cost.

The McCoy model utilizes a wound rotor. Here, a method of formulating power-equivalent permanent magnet machines is developed and the selection of wound or permanent magnet rotor is made random. This allows a determination of relative desirability between the two types based on how they are represented on the eventual non-dominated frontier.

The power rating (P) and rated mechanical rotational speed are constant for all motors synthesized. They comprise the basic customer requirements and are set to 40,000 hp and 168 rpm respectively, reflecting nominal per-shaft values for current frigates and destroyers.

The series and/or parallel connections of the rotor and stator poles are not specified. Calculations are performed on a per-turn basis as is common in preliminary design, although multiple rotors and stators are assumed to be connected in series. Therefore, while separate variables for the number of stages (n), the number of series stators (ss) and the number of series rotors (sr) appear in the equations to follow, their values are identical in the design code. The power factor angle is constant at 5 degrees lagging, or 0.0873 radians (inductive load) for all motors.

Specific cooling systems are not modeled. Motors are evaluated based on a heat density calculation, which provides a measure of the relative difficulty involved in heat removal. Shafts are designed with hollow centers to allow a flow path for forced gas or liquid cooling.

In designing electric motors to a given power rating, a common method employed is to set the peak flux density to some value at or below the saturation limit of the material used for the flux path and to perform the remaining calculations based on this value. In a typical three-phase electric machine, the highest flux density occurs in the steel teeth of the stator. Here, the maximum flux density in the stator teeth is allowed to vary between 1.0 and 1.9 Tesla, with the upper limit chosen to approach the saturation point of typical electrical steel.

Structural steel elements, which include the shaft, the casing and the portions of the rotor and stator assemblies delivering torque are designed to 10^8 N/m^2 shear stresses. This is approximately 1/3 of the yield strength of typical structural steel [5],[6]. The safety factor thus provided allows the motors to accommodate transient forces associated with marine propulsion.

The slot packing factor, or ratio of cross-sectional conductor area to slot area, is assumed to be 0.7 for the stator and 0.8 for the rotor. These are reasonable upper limits given common winding configurations and probable voltage ranges for these motors. Copper conductors are limited to a maximum current density of 10^7 A/m^2.[†]

2.2 Design Parameters

To develop a design code that produces random motors, it is first necessary to isolate a set of independent design parameters. These constitute the random or pseudo-random set of inputs to be generated at the beginning of each iteration. This set must be complete, or in mathematical terms, these state variables must span the design space. To allow random determination, the parameters must be limited to some finite range. These ranges were initially selected somewhat arbitrarily, taking feasible upper and lower limits into account where applicable and using judgment and expert advice when obvious limits did not exist. Later, during trial runs of the code, ranges were adjusted to generously bracket the normal distributions of the parameters on the frontier. This approach maintained the creativity of the routine while disallowing parameter values that produced exclusively dominated or infeasible designs.

In order to decrease processing time, only discrete incremental values of the continuous parameters are allowed. Table 2-1 summarizes the parameters selected, their ranges and increments.

[†] Current densities of this magnitude in copper cannot be cooled by forced air alone.

Table 2-1: Design Parameters

Design Parameter	Symbol	Lower Limit	Upper Limit	Increment
air gap width	g	1 mm	11 mm	1 mm
disk inner radius	R_i	0.50 m	1.80 m	0.1 m
disk outer radius	R_o	R_i^+	2.0 m	0.1 m
max stator tooth flux density at inner radius	B_{ti}	1.0 T	1.9 T	0.1 T
number of pole pairs	p	1	40	1
number of rotor slots per pole	q_r	1	9	1
number of rotor/stator pairs	n	1	30	1
number of stator slots per pole per phase	q_s	1	3	1
permanent magnet angle subtended	β	90 elec deg	180 elec deg	10 elec deg
rotor type	M	0 = wound	1 = magnet	-
stator slot fraction at disk inner radius	λ_{si}	0.2	0.8	0.1
stator slot height	h_{ss}	1 cm	11 cm	1 cm
stator winding pitch	*pitch*	0.7	1.0	0.1
wound rotor slot factor at disk inner radius	λ_{ri}	0.2	0.8	0.1
wound rotor slot height	h_{sr}	1 cm	11 cm	1 cm

2.3 Preliminary Calculations

Hereafter, random design parameters from Table 2-1 appear in ***bold italic***.

The apparent power of the motor (S) is a function of the power rating (P) and the power factor angle (ϕ), both of which are constant for all motors synthesized:

$$S = \frac{P}{\cos(\phi)} \quad volt \cdot amps$$

Rated mechanical frequency (ω_m) is given by:

$$\omega_m = \frac{rpm \cdot 2\pi}{60} \quad rad / s$$

where *rpm* is the rated mechanical rotational speed of the motor in revolutions per minute. Rated electrical frequency (ω_e) is a function of the number of pole pairs (p) and the rated rotational speed:

$$\omega_e = \frac{rpm \cdot 2\pi \cdot p}{60} = \omega_m p \quad electrical\ rad / s$$

Torque required per disk (T) is determined from the power rating, the mechanical frequency and the number of rotor/stator pairs, or *stages* (n):

$$T = \frac{P}{\omega_m \cdot n}$$

To proceed with the design calculations, it is convenient to define a disk *slot fraction.* The slot fraction (λ) is the ratio of the rotor or stator slot width to the distance between slots, or equivalently the total width of all slots divided by the total circumference. It is determined by the number of slots per pole per phase (q) and the number of pole pairs (p). In order to better understand the calculation of the slot fraction as a function of these parameters, it is helpful to become familiar with the disk geometries they specify. Figure 2-1 shows the disk configurations of one phase of a three-phase winding for various values of q and p, using an arbitrary slot width.

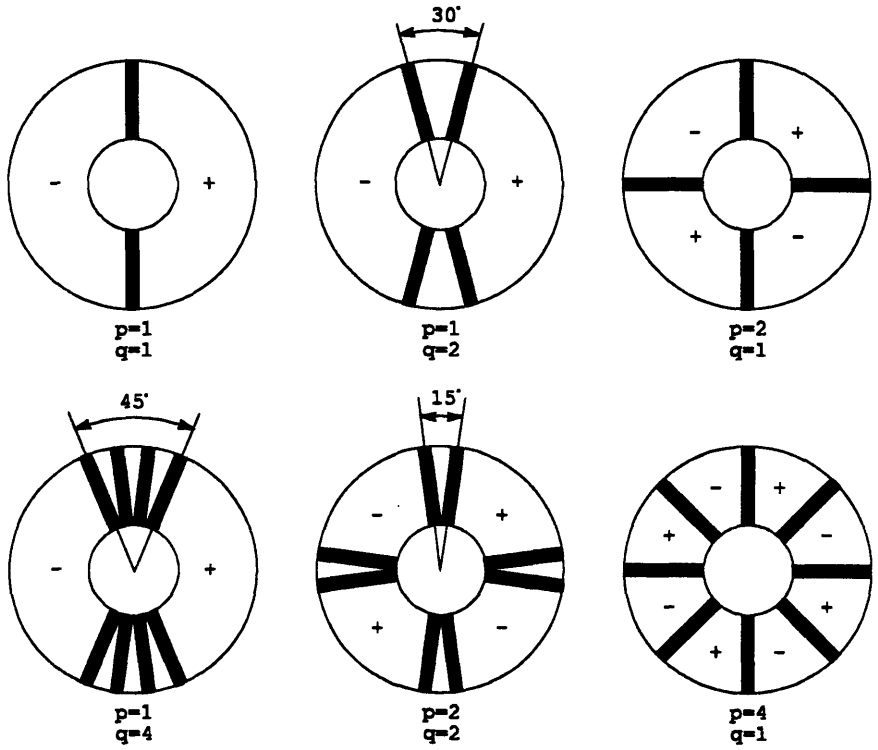

Figure 2-1: 3-Phase Disk Geometries

All slots in the figure (the black bars) are arranged for full pitch windings in order to simplify the diagrams. The winding turns, which consist of copper conductors surrounded by insulating material, will lie in these slots. A single series winding turn will loop around one positive pole face *and* its associated negative pole face, traveling in opposite directions around the two faces and describing somewhat of a figure eight. It will require at least two physical slots per pole pair, depending on whether and to what extent it is further split into parallel turns. By convention, these two *physical* slots are referred to as one (dual) "slot" per pole pair (q). This number of "slots" per pole pair actually indicates the distribution or *chording* of the winding over a pole face. Chording results in q magnetic axes for each pole, or q voltage phasors displaced by an angle of 60 electrical degrees divided by q. The resulting phasor magnitude is given by vector addition. Again

by convention, q is normally referred to as simply the number of slots per pole rather than the number of slots per pole pair. Thus if one wishes to count the number of physical slots present on a disk, it is necessary to multiply the product of the number of slots per pole (pair) and the number of pole pairs by a factor of two. Finally, for a multi-phase machine, the chording of the winding is represented by the number of slots per pole *per phase* and the calculation of the number of physical slots is adjusted accordingly. Thus for a three-phase axial machine stator, the slot fraction is:

$$\lambda_s(r) = \frac{w_{ss} \cdot q_s \dfrac{\text{"slots"}}{\text{pole pair phase}} \cdot 3\,\text{phase} \cdot \dfrac{2\,\text{slots}}{\text{"slot"}} \cdot p\ \text{pole pairs}}{2\pi r}$$

$$= \frac{6 q_s p}{2\pi r} \cdot w_{ss} \qquad r \geq R_i > 0$$

where w_{ss} is the stator slot width. For the single phase rotor,

$$\lambda_r(r) = \frac{2 q_r p}{2\pi r} \cdot w_{sr} \qquad r \geq R_i > 0$$

where w_{sr} is the rotor slot width. If the slot fraction is specified at some radius (the disk inner radius is the most convenient), the slot width is determined. For the stator,

$$\lambda_s(R_i) \equiv \lambda_{si}$$

$$w_{ss} = \frac{2\pi R_i}{6 q_s p} \cdot \lambda_{si}$$

and for the rotor,

$$\lambda_r(R_i) \equiv \lambda_{ri}$$

$$w_{sr} = \frac{2\pi R_i}{2 q_s p} \cdot \lambda_{ri}$$

Slot width is constant, but the tooth width of an axial machine increases with radius (the teeth are the spaces between the slots in Figure 2-1). Tooth width may also be defined in terms of q and p. For the stator:

$$w_{ts}(r) = \frac{2\pi}{6 q_s p}(r - R_i \lambda_{si})$$

Since the tooth width and therefore the permeable area available to the air gap flux is a function of radius, flux density in the tooth is also a function of radius (the insulation surrounding the conductors in the slots is considered to be essentially impermeable). The

point of maximum tooth flux density occurs at the disk inner radius. If the peak flux density in the gap is B_g, then the flux density anywhere in a stator tooth is given by:

$$B_{ts}(r) = \frac{B_g}{\left(\frac{w_{ts}(r)}{w_{ts}(r) + w_{ss}}\right)} = B_g\left(\frac{r}{r - R_i\lambda_{si}}\right)$$

The tooth flux density at the inner radius is used here as a design parameter (B_{ti}). As mentioned in the introduction to this section, it is allowed to vary but may not exceed the saturation value of the tooth material (1.9 Tesla). The peak value of the air gap flux density wave is determined when B_{ti} is specified:

$$B_{ts}(R_i) = B_g\left(\frac{1}{1-\lambda_{si}}\right) \equiv B_{ti}$$

$$B_g = B_{ti}(1-\lambda_{si})$$

2.4 Stator Calculations

2.4.1 Winding Factors

The stator breadth factor (k_{bs}) is an adjustment for the effect of chording. It is the reduction factor for the resulting voltage phasor of such an arrangement as compared to that of a concentrated winding [7]:

$$k_{bs} = \frac{\sin\left(\frac{q_s\gamma}{2}\right)}{q_s \sin\left(\frac{\gamma}{2}\right)} = \frac{0.5}{q_s \sin\left(\frac{\pi}{6q_s}\right)}$$

where γ, the electrical angle spanned by adjacent slots, is $\pi/3\mathbf{q_s}$ for a three-phase machine.

The stator pitch factor (k_{ps}) is a measure of the flux linked by a winding as compared to that which would be linked if the winding were full-pitched, i.e., if its turns spanned 180 electrical degrees. The derivation of its formula is also found in [7]:

$$k_{ps} = \cos\left(\frac{\pi(1-\mathbf{pitch})}{2}\right)$$

The effects of the breadth and pitch factors are normally combined in equations for preliminary design [8]. The total effect on flux linked and voltage generated is represented by their product, the winding factor (k_{ws}):

$$k_{ws} = k_{bs} k_{ps}$$

2.4.2 Flux Density, Voltage and Current

Flux density in the air gap is assumed to be of the form

$$B(\theta_m, t) = B_g \sin(p\theta_m - p\omega_m t)$$

where the peak value B_g has been determined in the preliminary calculations as a function of the maximum tooth flux density. The flux per pole is calculated by integrating this flux density over the area of a pole, which is bounded by the disk inner and outer radius and subtends a mechanical angle of π/p radians, or 180 electrical degrees:

$$\Phi = \int_0^{\pi/p} \int_{R_i}^{R_o} B(\theta_m, t)\, r\, dr\, d\theta$$

$$= \frac{(R_o^2 - R_i^2) B_g \cos(p\omega_m t)}{p} \quad Webers$$

Flux linkage (Λ) is then

$$\Lambda = \Phi \cdot N_s \cdot ss \quad Weber \cdot turns$$

where N_s is the number of series winding turns per stator and ss is the number of stators connected in series. Their product $N_s \cdot ss$ is the total number of series turns in the machine (since *all* stators are assumed to be connected in series for this study, ss is equal to the number of rotor/stator pairs n). Omitting the number of turns from the calculation, as is often done in preliminary design, results in a value of flux linkage *per turn*. Note that the distribution of these turns among the stator poles is irrelevant, as all turns link the same flux. Of course, this is only true if all turns are full pitched and concentrated, but this discrepancy is resolved by including the winding factor. Thus the terminal voltage of the machine is given by:

$$V_a = \frac{d\Lambda}{dt} = \frac{p\omega_m k_{ws} (R_o^2 - R_i^2) B_g \sin(p\omega_m t)}{p} \quad volts / turn$$

$$= \frac{\omega_e k_{ws} (R_o^2 - R_i^2) B_g}{\sqrt{2} p} \quad rms\ volts / turn$$

where electrical frequency has now been substituted for mechanical frequency. Note that the result is in terms of phase (line to neutral) voltage rather than the line to line voltage normally specified in multi-phase machine ratings. Also note that this voltage is *independent of the number of turns*, simply because the number of turns has been omitted from the calculation. This seemingly trivial point will become important when calculating current densities.

The armature current may now be found in terms of the rated apparent power and the phase voltage:

$$I_a = \frac{S}{3V_a} \quad amp \cdot turns$$

and the base impedance to be used for per-unit calculations is:

$$Z_b = \frac{S}{3I_a^2} \quad ohms \,/\, turn^2$$

Next, in order to calculate armature loading and slot current densities, it is necessary to determine the total current in the slots. The total current entering and leaving each series stator is

$$I_s = \frac{I_a}{N_s \cdot ss} \quad amps$$

If one set of slots were present for each series turn on a stator, then the magnitude of the current in each slot would be equal to the magnitude of I_s. This, of course, is not necessarily the case. The number of slots present on a disk is a function of the number of slots per pole and the number of poles, both of which are independent design parameters in this study. Multiplying I_s by the ratio of series turns per stator per phase to the number of stator slots per phase gives the *percentage* of I_s in each slot. A ratio greater than unity indicates that each slot contains more than one series turn; non-integer values indicate some combination of parallel connections among slots and poles. As the determination of the actual connection scheme is not necessary in preliminary design, it is not examined further here. However, there is one additional consideration in determining total slot current: conductors of adjacent turns share a slot. This is evident in the simplified one pole-pair, one turn per slot winding configuration of Figure 2-2.

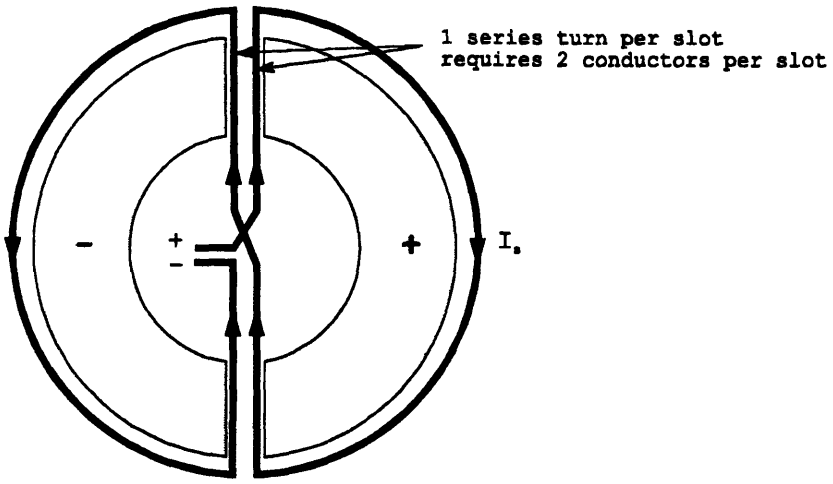

Figure 2-2: Simplified Winding Configuration

It can be seen from the figure that the fraction of I_s in a slot is actually twice the ratio mentioned above; this can be verified by picturing the conductor path necessary to complete the windings of any of the disk geometries in Figure 2-1. Thus the *total* current in a slot is:

$$I_{slot} = I_s \frac{2N_s}{N_{slots/phase}} = \left(\frac{I_a}{N_s \cdot ss}\right)\frac{2N_s}{q_s p} = \frac{6I_a w_{ss}}{\pi R_i \lambda_{si} ss} \quad amp \cdot turns$$

The armature electrical loading (K_a) is defined as the total current in each slot divided by the slot width:

$$K_a = \frac{I_{slot}}{w_{ss}} = \frac{6I_a}{\pi R_i \lambda_{si} ss} \quad amp \cdot turns / m$$

The slot current density J_{as} is then

$$J_{as} = \frac{K_a}{h_{ss}} \quad amp \cdot turns / m^2$$

where h_{ss} is the stator slot height, and the current density in the conductors is:

$$J_a = \frac{K_a}{h_{ss} \zeta_s} \quad amp \cdot turns / m^2$$

where ζ_s is the stator slot packing factor, or the ratio of conductor cross sectional area to slot cross sectional area. It is a function of the conductance of the winding insulation material used and the voltage in the conductors, and is assumed to be 0.7 for all motors generated in this study.

Since the calculated value of current density is independent of the number of turns, it may be compared to some maximum allowable conductor current density as a check on physical feasibility. The magnitude of the conductor current density is limited by the physical properties of the conductor material. Copper conductors are assumed for all motors generated in this study, allowing a maximum current density (using conventional cooling methods) of approximately 10^7 A/m^2. The calculated value of J_a is compared to this limit (J_{max} in the code) during the design synthesis. If J_a exceeds this value, the program increases the slot height and thus the conductor cross sectional area until current density is equal to J_{max}.

A second feasibility check is necessary. The prior assumption that the stator surface current density K_a is equal to the ratio of the slot current to the slot width becomes invalid if the slot height is much larger than the width, as do the leakage calculations that follow. There is no absolute definition of "much larger"; however, some limit must be imposed so that invalid slot geometries are not considered for evaluation. The slot height limit chosen in this study is three times the slot width. The synthesis of a motor whose slot height exceeds this is terminated and the motor is not evaluated.

2.4.3 Reactance

This section considers the combined effects of slot leakage and air gap reactance. Edge-turn leakage, skew and harmonics are assumed to have little impact on relative desirability.

Slot leakage reactance (X_{al}) is a result of flux that links the conductors themselves rather than entering the air gap. If the conductors in the slot are assumed to be distributed uniformly, then the magnetic field H transverse to the slot varies across the slot height [9]. A typical slot configuration is shown in Figure 2-3.

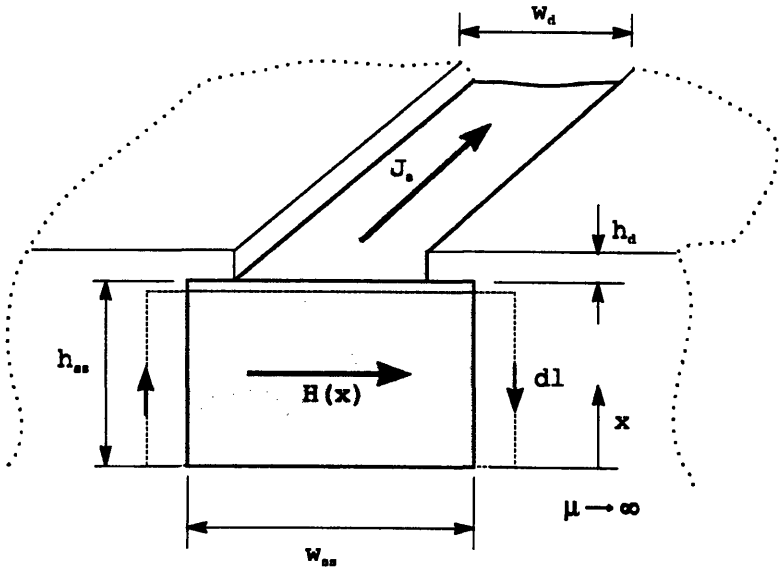

Figure 2-3: Slot Configuration

Applying the integral form of Ampere's Law to the path in the figure and using the previously defined slot current I_{slot} gives the magnetic field:

$$\oint_c \bar{H}(x)\cdot d\bar{\ell} = \int_s \bar{J}\cdot\hat{n}\,dA$$

$$H(x) = \begin{cases} \dfrac{I_{slot}}{w_{ss}}\dfrac{x}{h_{ss}} & 0 \le x \le h_{ss} \\ \dfrac{I_{slot}}{w_d} & h_{ss} \le x \le h_{ss} + h_d \end{cases}$$

The leakage flux above a conductor whose length is equal to that of the slot (R_o-R_i) and lying at a distance x above the bottom of the slot is

$$\Phi_{al}(x) = \mu_0(R_o - R_i)\int_x^{h_{ss}} \frac{I_{slot}}{w_{ss}}\frac{\hat{x}}{h_{ss}}\,d\hat{x} + \mu_0(R_o - R_i)\int_{h_{ss}}^{h_{ss}+h_d} \frac{I_{slot}}{w_d}\,d\hat{x}$$

$$= \mu_0(R_o - R_i)I_{slot}\left(\frac{h_{ss}^2 - x^2}{2h_{ss}w_{ss}} + \frac{h_d}{w_d}\right)$$

and the *average* flux above any conductor in the slot is

$$\bar{\Phi}_{al} = \frac{1}{h_{ss}}\int_0^{h_{ss}} \Phi_{al}(x)\,dx$$

$$= \mu_0(R_o - R_i)I_{slot}\left[\frac{h_{ss}}{3w_{ss}} + \frac{h_d}{w_d}\right]$$

so the total leakage flux linkage of a slot is the average flux multiplied by the number of conductors in the slot, which was calculated in the section on slot current density. Using this and the previous definition of I_{slot}:

$$\Lambda_{al} = \bar{\Phi}_{al}\frac{2N_s}{q_s p}$$

$$= \frac{4\mu_0(R_o - R_i)}{(q_s p)^2}\left[\frac{h_{ss}}{3w_{ss}} + \frac{h_d}{w_d}\right]\cdot N_s^2 I_s$$

If the slot depression h_d is assumed much smaller than the depression gap w_d, their ratio may be ignored. Note that this is an approximation, and also ignores the error introduced by neglecting the transition region between the slot and the depression. These effects are considered to be of second order and will have little impact on relative desirability among motors. Substituting the previously defined value of slot width and noting that there are $2q_s p$ slots per stator phase, the leakage reactance is given by:

$$
\begin{aligned}
X_{al} &= \frac{\omega_e \Lambda_{al}}{I_s} \\
&= \frac{4\omega_e \mu_0 (R_o - R_i) h_{ss} N_s^{\,2}}{3(q_s p)^2 w_{ss}} \\
&= \frac{4\omega_e \mu_0 (R_o - R_i) h_{ss} N_s^{\,2}}{q_s p \cdot \pi R_i \lambda_{si}} \quad \textit{ohms / slot} \\
&= \frac{8\omega_e \mu_0 (R_o - R_i) h_{ss} N_s^{\,2}}{\pi R_i \lambda_{si}} \quad \textit{ohms / stator} \\
&= \frac{8\omega_e \mu_0 (R_o - R_i) h_{ss} N_s^{\,2} \cdot ss}{\pi R_i \lambda_{si}} \quad \textit{ohms} \\
&= \frac{8\omega_e \mu_0 (R_o - R_i) h_{ss}}{\pi R_i \lambda_{si} \cdot ss} \quad \textit{ohms / turn}^2
\end{aligned}
$$

where the result has again been normalized with respect to the number of series stator turns in the machine.

The air gap reactance (X_{aa0}) corresponds to the self-inductance produced by the armature's own excitation. This may be calculated by considering the space fundamental component of magneto-motive force ($\mathcal{F}_{a1}$) produced by exciting a stator phase:

$$
\mathcal{F}_{a1} = \frac{4}{\pi} \frac{N_s k_{ws} I_s \cdot ss}{2p} \sin(p\theta_m)
$$

The resulting flux density in the air gap is:

$$
B_{a1} = \frac{4}{\pi} \frac{\mu_0 N_s k_{ws} I_s \cdot ss}{2 \cdot 2ng \cdot p} \sin(p\theta_m)
$$

where n is the number of stages (rotor/stator pairs) and g is the gap length, so $2ng$ is the total gap in the machine (each rotor in an axial machine requires two air gaps, one on either side). Integrating this flux density over the area of a pole gives the flux per pole:

$$
\begin{aligned}
\Phi_{aa0} &= \int_0^{\pi/p} \int_{R_i}^{R_o} B_{a1}(\theta_m)\, r\, dr\, d\theta \\
&= \frac{4}{\pi} \frac{\mu_0 N_s k_{ws} I_s ss}{4ngp} \frac{(R_o^{\,2} - R_i^{\,2})}{2} \frac{2}{p} \\
&= \frac{\mu_0 N_s k_{ws} I_s ss (R_o^{\,2} - R_i^{\,2})}{\pi ngp^2}
\end{aligned}
$$

The corresponding reactance is:

$$X_{aa0} = \frac{\omega_e N_s k_{ws} ss \Phi_{aa0}}{I_s}$$

$$= \frac{\omega_e \mu_0 N_s^2 k_{ws}^2 ss^2 (R_o^2 - R_i^2)}{\pi ngp^2} \quad ohms$$

$$= \frac{\omega_e \mu_0 k_{ws}^2 (R_o^2 - R_i^2)}{\pi ngp^2} \quad ohms / turn^2$$

The total synchronous reactance (X_d) for a three phase machine is

$$X_d = \frac{3}{2} X_{aa0} + X_{al} \quad ohms / turn^2$$

where the reactance due to phase-*a*'s own excitation is modified by the presence of the flux waves of phase-*b* and -*c*. These are each equal in magnitude to the phase-*a* wave but are space-displaced by ±120 electrical degrees.

The synchronous reactance is per-unitized as

$$x_d = \frac{X_d}{Z_b}$$

The steady state per-unit excitation voltage behind the synchronous reactance (e_{af}) and the internal power angle (δ) are determined by vector algebra:

$$e_{af} = \sqrt{1 + x_d^2 + 2x_d \sin\phi}$$

$$\delta = \sin^{-1}\left(\frac{x_d}{e_{af}}\right)$$

2.5 Rotor Calculations

Whether a particular motor synthesis will utilize a wound or a permanent magnet rotor is determined along with other design parameters at the beginning of each iteration. However, the rotor type does not impact the design module until the stator calculations are complete. At this point, the internal voltage and reactances have been determined and the rotor, whatever its type, is designed so as to satisfy these calculated values. The primary difference between the two types of rotor calculations is that a wound rotor is designed to produce the necessary internal voltage at a no-load condition. Field current under load is then a function of the rated internal voltage. For a permanent magnet rotor, however, the field flux density is constant and the rotor must be designed such that the internal voltage at rated conditions is the time derivative of the magnet flux.

2.5.1 Wound Rotor

Wound rotor windings are normally full pitch, as the harmonic-reducing benefits of fractional pitching are not realized with the DC rotor current. The rotor winding factor k_{wr} is therefore simply the rotor breadth factor, which is calculated in the same manner as for the stator:

$$k_{wr} = k_{br} = \frac{0.5}{q_r \sin\left(\frac{\pi}{6q_r}\right)}$$

No-load field current (I_{fnl}) is a function of the given air gap flux density:

$$B(\theta_m) = B_g \sin(p\theta_m) = \frac{4}{\pi}\frac{\mu_0 N_f k_{wr} I_{fnl} \cdot sr}{2 \cdot 2ngp}\sin(p\theta_m) \quad Tesla$$

$$B_g = \frac{\mu_0 N_f k_{wr} I_{fnl} \cdot sr}{\pi npg} \quad Tesla$$

$$I_{fnl} = \frac{\pi B_g npg}{\mu_0 k_{wr}} \quad amp \cdot turns$$

where N_f is the number of series turns per rotor (referred to the stator) and sr is the number of rotors connected in series so that the product $N_f \cdot sr$ is the total number of series field turns in the machine, referred to the stator. As with the stators, multiple rotors in this study are assumed to be connected in series, so that sr is numerically equivalent to the number of stages n.

Full load field current is the product of the no-load current and the rated per-unit internal voltage:

$$I_f = I_{fnl} e_{af} \quad amp \cdot turns$$

Rotor current densities may now be calculated. The current entering and leaving each series rotor is

$$I_r = \frac{I_f}{N_f \cdot sr} \quad amps$$

As in the stators, the fraction of this current in each rotor slot is twice the ratio of the series turns per rotor to the number of slots per rotor, and the slot current density is

$$J_{fs} = \frac{I_f}{N_f \cdot sr}\frac{2N_f}{q_r p}\frac{1}{w_{sr} h_{sr}}$$
$$= \frac{2I_f}{\pi R_i \lambda_{ri} h_{sr} \cdot sr} \quad amp \cdot turns / m^2$$

where the previous definition of w_{sr} has been used. Current density in the rotor conductors is:

$$J_f = \frac{J_{fs}}{\zeta_r} \quad amp \cdot turns / m^2$$

with the rotor slot packing factor ζ_r assumed to be 0.8, as compared with the value of 0.7 used for the stator. A larger packing factor is possible in the rotor slots due to the lower current magnitude in the field winding. As with the stator current densities, the calculated value of J_f is compared to the limiting value and rotor slot height is increased if necessary. This new slot height is then evaluated for feasibility based on the same slot width criterion.

2.5.2 Permanent Magnet Rotor

If each pole of the rotor is fitted with a magnet extending from the inner to the outer radius and subtending an angle of β, where $\beta \leq \pi/p$, then the space fundamental of the resulting flux density wave is:

$$B_{mag}(\theta_m) = \frac{4}{\pi} B_r \sin\left(\frac{p\beta}{2}\right)\frac{h_m}{h_m + 2g}\sin(p\theta_m)$$

where B_r is the residual flux density of the permanent magnet material and h_m is the height (thickness) of the magnet.[†] The flux per pole is then:

$$\Phi_{mag} = \frac{4}{\pi} B_r \sin\left(\frac{p\beta}{2}\right)\frac{h_m}{h_m + 2g}\int_0^{\pi/p}\int_{R_i}^{R_o}\sin(p\theta_m) r\, dr\, d\theta$$
$$= \frac{4}{\pi} B_r \sin\left(\frac{p\beta}{2}\right)\frac{h_m}{h_m + 2g}\frac{(R_o^2 - R_i^2)}{p} \quad Webers$$

The internal voltage is the time derivative of the flux linkage:

$$E_{af} = \omega_e \Phi_{mag} N_s k_{ws} \cdot ss$$
$$= \omega_e \Phi_{mag} k_{ws} \quad volts / turn$$

[†] The permanent magnet material assumed in all calculations is representative of relatively advanced commercial products available at the time of this writing, and has a residual flux density of 1.29 Tesla.

The ratio involving magnet thickness and gap length may be expressed in terms of the internal voltage, which is known from the stator calculations (note: $E_{af} = e_{af} \cdot V_a$):

$$\frac{h_m}{h_m + 2g} = \frac{E_{af}\pi p}{4\omega_e B_r \sin\left(\frac{p\beta}{2}\right) \cdot (R_o^2 - R_i^2) k_{ws}}$$

The value of air gap reactance has also been determined in the stator calculations. Therefore the *effective* air gap length is fixed, but it is now composed of a new (smaller) *actual* air gap and the thickness of the magnet (the permeability of the magnet material is assumed to be approximately equal to that of free space):

$$X_{aa0} = \frac{2\mu_0 \omega_e k_{ws}^2 (R_o^2 - R_i^2)}{\pi (h_m + 2g) n p^2}$$

$$\therefore \quad h_m = \frac{2\mu_0 \omega_e k_{ws}^2 (R_o^2 - R_i^2)}{X_{aa0} \cdot \pi n p^2} - 2g$$

Substituting this into the previous equation relating magnet thickness and air gap gives a new gap length g and the magnet thickness. A negative value for the new gap length is possible but not feasible; this requires another feasibility check on the synthesis. Any design with a negative gap length at this point is terminated. However, since this check is not necessary for a wound rotor machine, the iteration following a negative gap motor is forced to permanent magnet so that the number of both types of designs considered on average is equal.

2.6 Edge Turns

In radial gap machines, the paths taken by the conductors at the ends of the rotor and stator cylinders are known as end turns. The end turns are an unfortunate consequence of the fact that the return path of a winding turn must be displaced azimuthally from its initial path in order to form a loop and link flux. The angle of displacement is determined by the number of poles, the number of slots per pole and the winding pitch. End turns serve to close the winding coils at each end of the machine but do not contribute to the torque developed. It is common to seek methods of minimizing the curvilinear length of the end turns in order to reduce resistance losses and increase overall machine efficiency. End turns also tend to increase machine volume because a stacking effect occurs as the windings are installed.

The impact of the end turn geometry on machine volume and efficiency generally increases with the power rating; the configuration chosen for low-torque machines has little effect on these attributes. Several methods of optimizing the end turn configuration for high-torque machines are in use, and non-conventional methods such as the helical winding proposed by J. L. Kirtley can result in tangible benefits in efficiency and volume [10].

The equivalent of end turns in axial gap machines might more precisely be called edge turns. Rather than traveling over the flat ends of a cylinder as in a radial machine, the conductors in an axial machine must traverse a given angle about the inner and outer periphery of the disk. Simplified diagrams comparing the two types of geometries are shown in Figure 2-4.

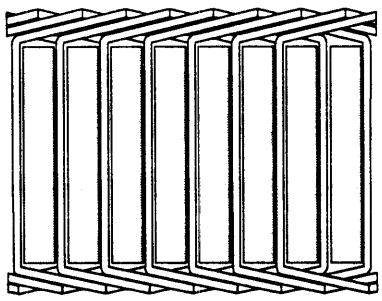

Radial Machine Winding (Laid Flat)

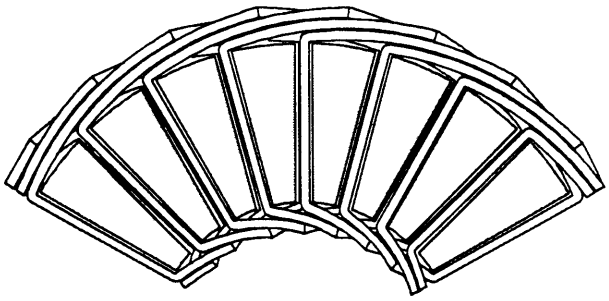

Axial Machine Winding

Edge View

Figure 2-4: Winding Geometries

In both motor types, the conductors must exit a slot at some non-zero angle in order to avoid the conductor exiting the adjacent slot. For the radial machine, the angle of the conductor with respect to the teeth is constant and the resulting form of the end turn, assuming that the conductors must stack, is triangular. For the axial machine, this stacking requires the conductor's radial coordinate to change continuously and the *rate* of change, rather than the angle itself, is constant. This condition is expressed mathematically in terms of the conductor path's coordinates as:

$$\frac{dr}{d\theta} = constant$$

This constant may be further investigated by considering the situation at the disk inner radius in Figure 2-5.

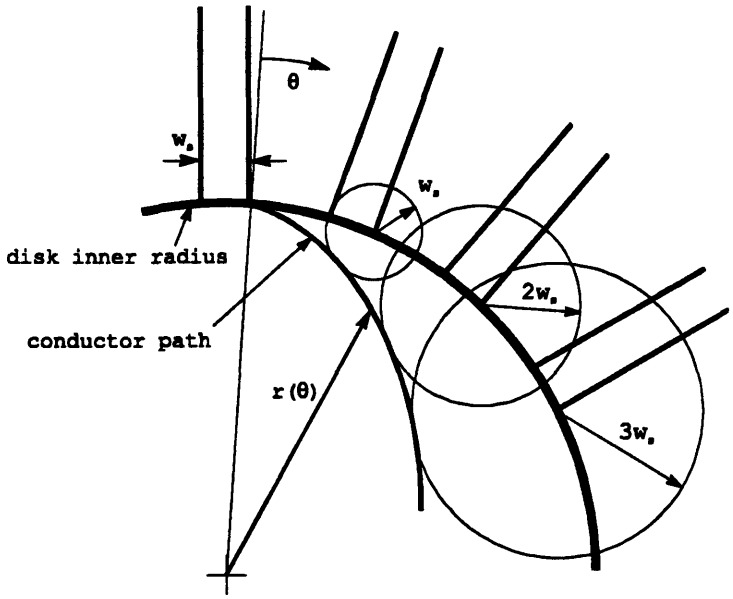

Figure 2-5: Inner Edge Turn Path

The conductor path shown in the figure is actually the outer edge of the conductor exiting the topmost slot. The circles centered on the disk inner radius are of radius $m \cdot w_s$, where m is the number of slots removed from the path's exit point. The shortest path available for the conductor, if it is to clear the conductors exiting the intermediate slots, is the curve tangent to these circles.

Upper and lower bounds on the constant rate of change of the conductor path may be obtained by considering Figure 2-6, where the path encounters the conductor exiting the adjacent slot.

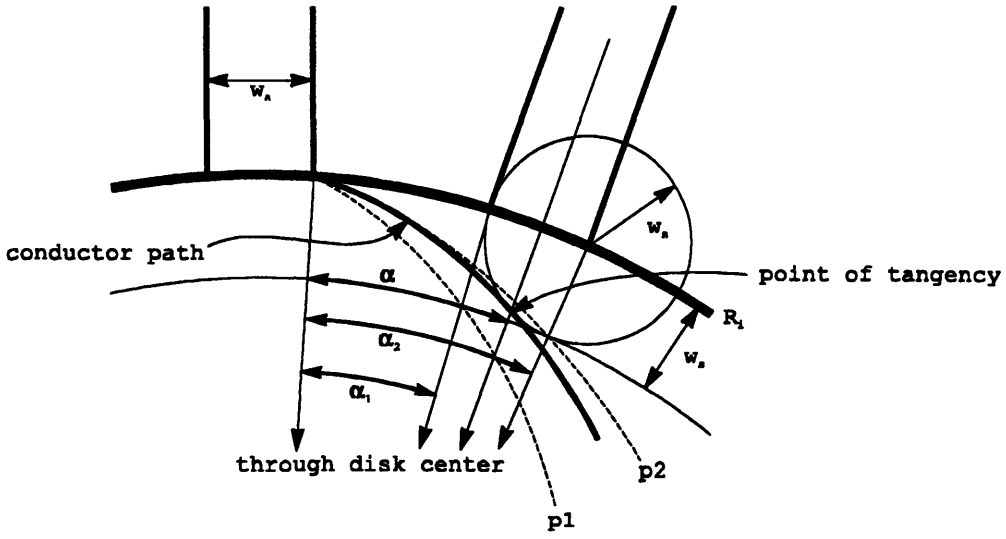

Figure 2-6: Edge Turn Path Bounds

If the conductor's radial coordinate decreases by a slot width (w_s) while traversing the angle α_1, the conductor follows path p1 and travels inside the tangency point. If a radial decrease of one slot width occurs over the angle α_2, the conductor follows path p2 and travels outside the tangency point. The actual curve tangent to the circle lies between these paths. The angles may be defined in terms of their distances spanned on the inner radius, as α_1 subtends a tooth width and α_2 subtends the sum of a tooth width and a slot width:

$$\alpha_1 = \frac{w_t(R_i)}{R_i} = \frac{w_s(1-\lambda_i)}{R_i\lambda_i}$$

$$\alpha_2 = \frac{w_s + w_t(R_i)}{R_i} = \frac{w_s}{R_i\lambda_i}$$

The subscripts *s* and *r* denoting stator and rotor are omitted from the variables throughout this section as the analysis applies to either. The actual angle α subtended by the path while undergoing a radial change of one slot width must lie between α_1 and α_2; that is, the conductor must reach a distance of one slot width from the disk inner edge at some point *between* the boundaries of the next slot. Thus:

$$\alpha = \frac{w_s}{R_i\lambda_i}\xi \qquad 1-\lambda_i < \xi < 1$$

with ξ yet to be determined.

Since the rate of change of all conductors is equal and constant, the tangency point must be a function of the initial exit angle from the slot. The complement of this exit angle (Γ) is shown in Figure 2-7.

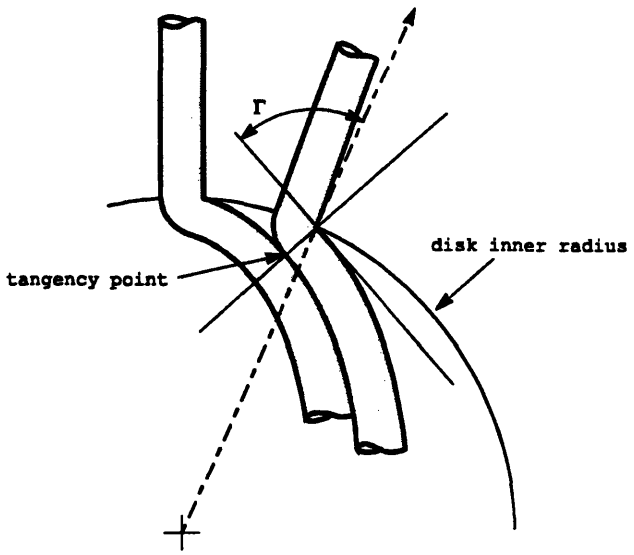

Figure 2-7: Conductor Exit Angle

The angle Γ may be defined in terms of the conductor's rate of change at the disk inner radius [11]:

$$\frac{dr}{d\theta} = \frac{-R_i}{\tan\Gamma}$$

Using the exit angle as a parameter, the radial coordinate of the tangency point may be estimated. A detailed view of the situation as the conductor path encounters the adjacent slot is shown in Figure 2-8.

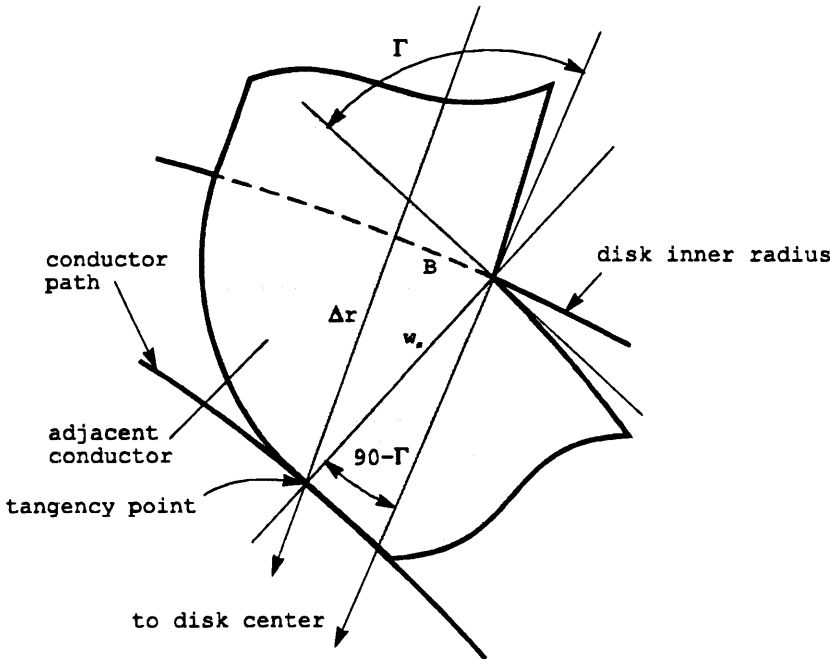

Figure 2-8: Detail of Tangency Point

The radial distance Δr between the disk inner radius and the tangency point may be approximated by

$$\Delta r \cong w_s \cos(90°-\Gamma) = w_s \sin\Gamma$$

Chord B in the figure is given by

$$B \cong w_s \sin(90°-\Gamma) = w_s \cos\Gamma$$

The angle α from before may now be approximated by adding the angles subtended by the tooth and the slot and subtracting the angle subtended by the chord B:

$$\alpha \cong \left(\frac{w_t(R_i) + w_s - w_s \cos\Gamma}{R_i} \right) = \frac{w_s}{R_i} \left(\frac{1-\lambda_i}{\lambda_i} + 1 - \cos\Gamma \right) = \frac{w_s}{\lambda_i R_i} (1 - \lambda_i \cos\Gamma)$$

Equating this with the previous expression for α gives:

$$\xi = 1 - \lambda_i \cos\Gamma$$

and the conductor's rate of change must be

$$\frac{dr}{d\theta} \cong \frac{-\Delta r}{\alpha} = \frac{-w_s \sin\Gamma}{\left(\frac{w_s(1-\lambda_i \cos\Gamma)}{\lambda_i R_i} \right)} = \frac{-\lambda_i R_i \sin\Gamma}{1-\lambda_i \cos\Gamma}$$

Setting this equal to the previous expression for rate of change in terms of Γ gives:

$$1 - \lambda_i \cos\Gamma = \lambda_i \sin\Gamma \tan\Gamma$$
$$\cos\Gamma - \lambda_i \cos^2\Gamma = \lambda_i \sin^2\Gamma$$
$$\Gamma = \cos^{-1}\lambda_i$$

and therefore

$$\xi = 1 - \lambda_i^2$$

So the rate of change for the conductor becomes:

$$\frac{dr}{d\theta} = \frac{-R_i \lambda_i}{\sqrt{1-\lambda_i^2}}$$

Obviously, wide slots in close proximity (values of λ_i approaching unity) will result in large radial excursions by the conductors in the edge turns and will require significant margins at the disk edges to accommodate them. These margins, and the length of the turns themselves, must be accounted for in order to size the machine and calculate resistance losses correctly.

Integrating the above expression and specifying the constant results in an equation for the conductor path in polar coordinates:

$$r(\theta) = R_i \left(1 - \frac{\lambda_i \theta}{\sqrt{1-\lambda_i^2}} \right)$$

and the length of such a curve from slot exit to its maximum radial excursion at mid-span is given by G. Simmons [11]:

$$S = \int ds = \int_0^{\Psi} \sqrt{r^2(\theta) + \left(\frac{dr}{d\theta}\right)^2}\, d\theta$$
$$= \int_0^{\Psi} \boldsymbol{R}_i \sqrt{\kappa^2 + 1 - 2\kappa\theta + \kappa^2\theta^2}\, d\theta$$

where

$$\kappa = \frac{\lambda_i}{\sqrt{1-\lambda_i^2}}$$

and Ψ is the angle between conductor exit and mid-span:

$$\Psi = \frac{1}{2} \cdot \frac{\pi}{\boldsymbol{p}} \cdot \boldsymbol{pitch}$$

The solution to integrals of this form may be found in various mathematical references, such as the *CRC* series [12]:

$$S = \boldsymbol{R}_i \left[\frac{(\kappa\theta - 1)\sqrt{\kappa^2 + 1 - 2\kappa\theta + \kappa^2\theta^2}}{\kappa} + \frac{\kappa}{2} \ln\left(2\sqrt{\kappa^4 + \kappa^2 - 2\kappa^3\theta + \kappa^4\theta^2} + 2\kappa^2\theta - 2\kappa\right) \right]_0^{\Psi}$$

At mid-span ($\theta = \Psi$), the conductor's rate of change reverses and it follows a mirror image of the initial path until it re-enters a slot. Thus the total length of a conductor inner edge turn (ℓ_i) is $2S$.

The radial thickness required for the edge turns is the difference in the disk inner radius and the conductor's radial position at mid-span:

$$\Delta R_i = \boldsymbol{R}_i - r(\Psi) + w_s$$
$$= \boldsymbol{R}_i - \boldsymbol{R}_i(1 - \kappa\Psi) + w_s$$
$$= \frac{\boldsymbol{R}_i \kappa \cdot \pi \cdot \boldsymbol{pitch}}{2\boldsymbol{p}} + w_s$$

The addition of the slot width w_s is necessary because the path has been integrated along the inner edge of the conductor. This calculation of the edge turn thickness, which depends only on preliminary design parameters, allows for another physical feasibility check on the motor. If ΔR_i is greater than $\boldsymbol{R}_i$, there is no space available for the shaft and the synthesis is terminated.

Analysis of the outer edge turns is similar. The conductor's initial rate of change is positive, and the turn length and maximum radial excursion are found by replacing R_i and λ_i in the above equations with R_o and λ_o (the slot fraction at the outer radius) given by

$$\lambda_o = \frac{R_i}{R_o}\lambda_i$$

The length of *half* a winding turn is the sum of the inner and outer edge turn lengths and twice the radial span of the disk. Since a single turn in an axial machine as defined in this study consists of two "loops" describing a figure eight around opposite poles, the total turn length L is twice this value:

$$L = 2\cdot\left[2(R_o - R_i) + \ell_o + \ell_i\right]$$

2.7 Structural

Since the edge turn stack thickness of the rotor and stator windings are not necessarily the same, the shaft and casing of the machine must be sized so as to accommodate the larger of the two values:

$$\Delta R_i = \max\left[\Delta R_{ri}, \Delta R_{si}\right]$$
$$\Delta R_o = \max\left[\Delta R_{ro}, \Delta R_{so}\right]$$

The stator disks are held motionless by the casing. The torque T acting on them creates a shear stress at the outer edge of the disks. Specifying a maximum allowable value of shear stress in the structural steel ($\tau_{max} = 10^8$ Pa throughout) determines the stator disk thickness as a function of the disk outer radius and the outer edge turn thickness:

$$t_s = \frac{T}{2\pi(R_o + \Delta R_o)^2 \tau_{\max}}$$

The rotor torque is transmitted to the shaft rather than the outer structure. Rotor thickness is therefore a function of the disk inner radius and the inner edge turn thickness, if the shaft is assumed to be as large as possible:

$$t_r = \frac{T}{2\pi(R_i - \Delta R_i)^2 \tau_{\max}}$$

So the shaft outer diameter is:

$$d_{so} = 2(R_i - \Delta R_i)$$

The shaft is modeled as a hollow tube subjected to torsional loading. The equation relating the applied torque to the shaft outer diameter is given by E. P. Popov [13]:

$$\frac{2I_p}{d_{so}} = \frac{torque}{\tau_{\max}}$$

where I_p is the polar moment of inertia:

$$I_p = \frac{\pi}{32}(d_{so}^4 - d_{si}^4)$$

and the torque on the shaft is the torque per disk T multiplied by the number of rotor disks $\boldsymbol{n}$. Sizing the shaft wall thickness such that maximum stress criterion is met gives the shaft inner diameter:

$$d_{si} = \left[d_{so}^4 - \frac{16T\boldsymbol{n}d_{so}}{\pi\tau_{\max}} \right]^{\frac{1}{4}}$$

Imaginary values of d_{si} indicate that even a solid shaft cannot carry the required torque and the design is infeasible. As with all other feasibility checks, shaft inner diameter is evaluated immediately upon calculation and the synthesis is terminated if the value is imaginary.

The shaft is also subject to static bending stresses due to the combined weight of the shaft itself and the attached rotors. The maximum bending stress is a function of the shaft material, the number and weight of the rotors, and the length of the shaft between supports. Bearings are assumed to be present only at the ends of the machine. The distributed weight per unit length on the shaft is:

$$w = \frac{\boldsymbol{n} \cdot W_r + W_{sh}}{sl} \quad kg / m$$

where W_r is the weight of a rotor, W_{sh} is the shaft weight and sl is the stack length of the machine (calculations of component weights and the machine's stack length are discussed in the following section). The maximum bending stress in a simply supported hollow shaft subjected to a distributed load is given by S. H. Crandall et al. [5]:

$$\sigma_{max} = \frac{sl^2 d_{so} w}{16 I_p}$$

The shaft outer diameter (d_{so}) and the polar moment of inertia (I_p) have been previously defined. This maximum stress is calculated and compared to τ_{max}. If necessary, the shaft is re-sized, keeping the outer diameter constant, until an acceptable value of stress is

obtained. If the shaft inner diameter reaches zero, the synthesis is terminated. Note that a Mises total stress analysis, allowing for simultaneous effects of torsion and bending, is not performed. This is justified by the safety margin inherent in the specification of τ_{max} and by the fact that bending stress is a static condition and is most prominent when the machine is at rest.

There is a third consideration involving the shaft dimensions. Even if torsional and bending stresses are satisfactory, it is possible that the maximum displacement of the shaft at rest is excessive. Such "bowing" of the shaft when the machine is not in use will require lengthy warm-up procedures and can result in a permanent deformation, rendering the machine inoperative. The maximum displacement of the shaft at rest (δ_s) occurs at mid-span. Mid-span displacement of a simply supported hollow shaft subjected to a distributed load is given by Crandall et al. [5]:

$$\delta_s = \frac{w \cdot \left(\frac{sl}{2}\right)^4}{8 E_s I_p} \quad m$$

where E_s is the Young's modulus of the material and w is the distributed load. This displacement becomes a more useful parameter when expressed as a percentage of span. The resulting value is defined here as the shaft runout (*sro*):

$$sro = \frac{\delta_s}{sl}$$

If shaft runout exceeds the maximum value allowed (1% in this study), the shaft cross sectional area is again increased as necessary. As before, an adjusted shaft inner diameter of zero or less terminates the synthesis.

The outer structure of the machine is modeled as a hollow tube that must be capable of withstanding the torque required to hold the stators in place. This outer structure is the machine casing. The same equations used for sizing the shaft apply; however, the outer diameter must now be found in terms of the known inner diameter. This results in an implicit equation, and is resolved in the program by solving for roots and setting the outer diameter equal to the smallest real root that is larger than the inner diameter. Also, if the thickness of the shaft has been increased due to either the bending or runout criteria, the resulting casing thickness is increased in the same proportion.

2.8 Weight and Volume

All stages of an axial gap machine use the same back iron (perhaps more accurately called end iron or end steel) for the flux return path. It is composed of two equal volumes of electrical steel located at either end of the machine (see Figure 1-1). This end iron is in the form of disks in which parallel lines of flux travel azimuthally, and the disk thickness must

be such that saturation does not occur. The cross section of the end iron normal to the flux path is a rectangle of dimension $t_b \cdot (R_o - R_i)$, where t_b is the disk thickness. The total flux per pole in this cross section is equal to the total flux per pole in the air gap. The peak flux per pole in the air gap was previously calculated:

$$\Phi = \frac{R_o^{\,2} - R_i^{\,2}}{p} B_g$$

In the end iron, the peak flux per pole must be

$$\Phi_e = (R_o - R_i) t_b B_{sat}$$

Thus the required end iron thickness is determined:

$$t_b = \frac{B_g}{B_{sat}} \left(\frac{R_o + R_i}{p} \right)$$

Shaft and casing volumes and weights are straight-forward calculations based on the component dimensions and mass densities. The weights of the rotors and stators are determined from the volume of copper, insulation, electrical steel, and structural steel in each and their respective mass densities. The copper and insulation volume in a stator disk may be determined from the slot dimensions, the number of slots, the packing factor and the turn length:

$$\begin{aligned} Vols_{Cu} &= L_s h_{ss} w_{ss} \zeta_s \cdot 3 q_s p \cdot n \\ &= L_s h_{ss} \zeta_s \cdot \pi R_i \lambda_{si} \cdot n \\ Vols_{ins} &= Vols_{Cu} \left(\frac{1 - \zeta_s}{\zeta_s} \right) \end{aligned}$$

The volume of electrical steel required for the stator teeth ($Vols_{esteel}$) is found from the disk dimensions, the slot fraction and the slot height, with a factor of two included to allow a foundation for the teeth. The structural steel volume ($Vols_{ssteel}$) is simply the surface area of the disk multiplied by the previously calculated structural steel thickness:

$$\begin{aligned} Vols_{esteel} &= \pi (R_o^{\,2} - R_i^{\,2})(1 - \lambda_{si}) \cdot 2 h_{ss} \\ Vols_{ssteel} &= \pi (R_{os}^{\,2} - R_{is}^{\,2}) t_s \end{aligned}$$

Similar calculations result in rotor material volumes. If the rotor is a permanent magnet type, the magnet volume is found using the subtended angle β, the disk inner and outer radii and the previously calculated magnet thickness. The magnet mounts of a permanent magnet rotor are assumed to have a height equal to that of the magnet (h_m) and are modeled as the rotor "teeth". This allows the calculation of rotor electrical steel volume.

The overall machine length, or stack length, is found by simply summing the axial dimensions of all components:

$$sl = (2h_{ss} + t_s + 2h_{sr} + t_r + 2g) \cdot n + 2t_b$$

2.9 Losses

By far the most significant loss mechanism in an electric machine is the resistance of the copper conductors. The resistance of a single stator turn is:

$$R_t = \frac{L_s}{\sigma_{Cu} A_{cond}}$$

where σ_{Cu} is the conductivity of copper and A_{cond} is the cross sectional area of the conductor, which is the slot cross section multiplied by the packing factor and divided by the number of conductors in the slot:

$$A_{cond} = \frac{w_{ss} h_{ss} \zeta_s}{\left(\frac{2N_s}{q_s p}\right)} = \frac{\pi R_i \lambda_{si} h_{ss} \zeta_s}{6N_s}$$

The armature resistance per phase is then:

$$\begin{aligned} R_a &= R_t N_s \cdot ss \\ &= \frac{6N_s^2 L_s \cdot ss}{\sigma_{Cu} \cdot \pi R_i \lambda_{si} h_{ss} \zeta_s} \quad ohms \\ &= \frac{6L_s}{\sigma_{Cu} \cdot \pi R_i \lambda_{si} h_{ss} \zeta_s \cdot ss} \quad ohms / turn^2 \end{aligned}$$

and the total resistance loss in the armature is:

$$P_{La} = 3I_a^2 R_a \quad Watts$$

Field resistance loss for a wound rotor machine is found similarly. The core losses, due to hysteresis effects in the teeth and end iron, are not as easily determined. One method of approximating these losses is to obtain relevant manufacturer data for the material used and to curve fit a function of flux density and electrical frequency to the data. A fit that works well for silicon steel is given by Kirtley [14]:

$$P_C = P_B \left(\frac{B}{B_B}\right)^{\varepsilon_B} \left(\frac{\omega}{\omega_B}\right)^{\varepsilon_f}$$

where P_C is the power loss in the core per unit steel mass. Base values for typical electrical steel are:

$$P_B = 8.86 \, {}^{W}/_{kg}$$
$$\varepsilon_B = 1.88$$
$$\varepsilon_f = 1.53$$

Windage and friction losses are very small due to the low mechanical speed of the motors and are not calculated. Machine efficiency is determined in the usual way as a function of input power and total losses.

3. Machine Attributes and Naval Architecture

The identification and evaluation of decision-impacting product attributes are the most crucial aspects of the Novice method when used for optimization. The attributes that have an impact on the selection process, and are therefore candidates for evaluation, are dependent upon the product's intended use. For example, the list of desirable electric motor attributes for general commercial use would not be significantly different from one application to another, and would most likely include rated efficiency and acquisition cost in particular. Specialized applications, such as military use, may require additional or modified characteristics. Whatever the application, a complete list of the attributes that may influence the customer's choice is essential in order to begin the evaluation process. To the greatest extent possible, this list should be non-redundant and non-contradictory. These qualities are of importance because they influence the size of the non-dominated frontier; their impact is discussed further in Chapter 4. The determination of applicable attributes in applying axial gap motors to warship propulsion is the subject of this chapter.

3.1 Needs of the Navy

Since warship propulsion may be considered a specialized application for an electric motor, the criteria by which such a motor's relative usefulness are judged differ from those of a motor intended for general use. Size and weight become much more critical, and depending on a ship's internal arrangement, may exceed overall efficiency in terms of significance. Size serves as an example of how the list of attributes selected for evaluation may differ among applications. The Navy would normally prefer the smallest motor possible (for several reasons, which are addressed in this chapter); size therefore becomes an attribute of evaluation. Commercial customers, on the other hand, would normally not be excessively concerned with the physical dimensions of the motor as long as they were within reasonable limits. In their opinion, smaller would not necessarily be better. This might simply dictate an upper bound on size; it would probably be implemented as a feasibility check rather than evaluated for optimization. Thus the total number of relevant attributes for a Navy application would be larger than for commercial use. In general, it can be assumed that the number of attributes to be evaluated will increase with the specialization of the intended application.

Other than size, characteristics which are important in Navy propulsion but do not normally impact commercial motor design include noise level, the ability of the motor to operate in a damaged condition, resistance to shock, adaptability to a marine environment (e.g. resistance to chloride corrosion), and the effect of the motor's radius on the propeller shaft angle. These and other relevant factors are discussed individually in their respective sections.

Some of the characteristics that will be identified as relevant here (such as weight and size) are determined in preliminary design. Others, such as life cycle cost, are quantifiable but

are influenced by factors external to the design (discount rate, fluctuating price of fuel, expected length of life cycle, etc.). Still others, such as robustness and noise level, are normally determined from testing and performance data. They may be a functions of other motor attributes and difficult to quantify from a preliminary design standpoint. Of the three types, the exactly defined attributes are of course the simplest to evaluate, particularly when they have an obvious optimum value. Attributes that are affected by external factors present greater difficulty and may require assumptions or predictions; however, as long as the assumptions are reasonably accurate the frontier will be unaffected if they are applied equally to all motors. The third type presents the greatest difficulty. Attempting to calculate a noise level, for example, and using it as a comparison attribute will certainly impact the eventual frontier. If the algorithm is incorrect or incomplete, the frontier will be incorrectly skewed but this will not be obvious from the results. Attributes in this category must be considered carefully before they are inserted into the optimization process. In some cases they may be omitted with the understanding that there will be opportunities to subjectively screen the designs on the frontier after the process is complete.

3.2 Formulation of Motor Attributes

The motor attributes selected for consideration and discussed in the following sections are a result of the author's experience in naval architecture and on Navy ships, in addition to interviews with experienced designers and arrangers in Navy labs and commercial facilities. Care is taken to include all reasonable attributes at least for purposes of discussion; in some cases the attribute's impact on *relative* usefulness is judged insignificant or the quantification is subjective enough that it is omitted from the evaluation process. For quantifiable attributes, the reasons for their importance and their methods of calculation are given.

3.2.1 Weight

The weight of the motor affects the ship's displacement. Ships are designed to float at a given draft and the net weight of the ship's structure and outfitting must remain relatively constant over its lifetime. Decreasing the weight of required structure or machinery components (such as propulsion motors) allows for an increase in weight elsewhere (and vice versa). This weight reduction may be made up by increasing the fuel capacity, thus increasing the ship's endurance range, or by adding more armament, thus increasing the payload fraction and the ship's fighting capability (payload fraction is normally defined as the ratio of the total weapons and surveillance systems weight to the ship's full load displacement). In addition, a heavier motor will require a stronger foundation. This will result in a further increase in net weight, if additional structure is added, or an increase in acquisition cost if the foundation is modified by using stronger materials.

The motor weight also impacts internal arrangements. Since it will almost certainly be placed at some point other than the ship's center of gravity, it will affect trim, heel and stability. Trim is a measure of a ship's static longitudinal departure from level, and is

defined as the difference in the ship's draft (the distance from the keel to the waterline) forward and aft. For example, a ship floating at a draft of 19 feet measured at the bow and 18 feet measured at the stern is said to be trimmed 1 foot by the bow. The dynamic counterpart of trim is pitch. Heel, or list, is a measure of static inclination about the longitudinal axis; it is given in degrees port or starboard. The dynamic counterpart of heel is roll. A relatively massive motor may not be placed as far from the center of gravity as a relatively light motor for given values of trim and heel.

Obviously, a motor of low weight is desirable in terms of its impact on these factors. As there is no lower limit on the weight of motors generated in the synthesis, the optimum value of weight is considered to be zero.

3.2.2 Volume

A ship's internal volume, even more so than weight, is a given constant. Analogous to the weight arguments above, the reduction in volume of any internal component allows for more volume elsewhere, whether it be in fuel, weapons, or living space. Thus small motor volume is desirable and the optimum value of motor volume is considered to be zero.

3.2.3 Rated Efficiency

A high value of rated efficiency is an obviously desirable trait in any motor, regardless of application. Although its impact on the selection of a motor for use in warship propulsion is relatively minor compared to the *average* efficiency (see the life cycle cost section below), it remains an indicator of the quality of a design and is a useful attribute for optimization. It is calculated as the ratio of the output power to the input power, or equivalently the ratio of input power minus the total losses to the input power, at rated conditions. Its optimum value is considered to be 100%.

3.2.4 Heat Density

The fact that axial gap machines are volume efficient relative to radial machines makes them more difficult to cool. This has been the primary obstacle to their implementation, and was the focus of McCoy's work. As he pointed out in his conclusions, his proposed radial thermosyphon method, although promising, "cannot yet be recommended without reservations" [1]. Liquid cooling and cryogenics, among other methods, have also been considered without complete success. It is not the purpose of this study to solve the cooling problem in axial machines; rather, it is to determine which machines, if they *can* be cooled, are the best for Naval propulsion. In this light, it is sufficient to obtain some measure of the difficulty expected in cooling the machines. This is accomplished by calculating the motor's heat density:

$$h_{dens} = \frac{P_L}{Vol_m}$$

where P_L is the total first order power loss (resistance plus core) at rated conditions and Vol_m is the machine volume. High values of heat density will require extensive and possibly complex cooling systems as discussed in Chapter 1, thus increasing the cost and decreasing the reliability of the propulsion system. The optimum value of heat density is considered to be zero.

3.2.5 Cost

Monetary cost, like rated efficiency, is an obvious attribute for evaluation. The monetary cost considered here is total life cycle cost, which is the sum of acquisition and operational costs over the motor's lifetime.

3.2.5.1 Acquisition Cost

Acquisition cost is the monetary outlay required to obtain the motor. It is expressed in terms of current dollars at the time of acquisition and is the sum of a motor's material cost, construction cost, and the manufacturer's profit.

3.2.5.1.1 Material Cost

The total cost of materials for a given machine (C_{mat}) is easily calculated in preliminary design using the volumes of the various materials in the motor and their market costs. Table 3-1 summarizes the materials used here and their approximate costs at the time of this writing[†]:

Table 3-1: Materials and Costs

Material	Cost ($/kg)
structural steel	0.90
copper	2.20
insulation	9.00
electrical steel	1.15
magnet material	130.00

The acquisition cost of a motor will also include the cost of power electronics. The relevant characteristics of power electronics in terms of naval architecture (cost and volume) are primarily functions of the electronics' power handling capacity. Power electronics are normally classified by their power handling capacity per unit volume and per unit cost. The maximum switching speed at rated power may also be of importance. The required switching capability is determined by the motor's rated rotational speed and the number of poles. As either of these values increases, the frequency of the input voltage and thus the switching speed of the electronics also increases. However, the rated rotational speed is constant for all motors in this study (168 rpm). For a one pole-pair

[†] These costs are variable and should not be used for calculations without updating. The magnet material is representative of Crucible Magnetics Corporation's CRUMAX® 4014 line.

motor, this requires input voltage at 2.8 Hz. Even for 40 pole-pairs, the maximum number allowed in this study, the required frequency is only 112 Hz. This is well within the capability of electronics currently used aboard ships. In contrast, the predicted switching capability of the next generation of power electronics is approximately 100 kHz [4]. The range of switching speed required by these motors is therefore 0.1% of projected capability, and it is reasonable to assume that variation over this range will not affect the electronics cost. Since all motors also have identical rated powers, the cost (and volume) of electronics should not affect comparisons and is therefore not included.

3.2.5.1.2 Construction Cost

Construction cost is calculated using the price of construction labor and the time required to assemble and test the machine. Axial gap motors are not in production at the time of this writing in the power range required for Navy propulsion; no production history exists on which to base construction cost estimates. The largest working device produced to date is a single stage 2780 hp prototype built by Kaman Electromagnetic Corporation for the Navy in 1994. This prototype utilized a permanent magnet rotor. Research into its fabrication process was used to formulate an approximate construction cost model for axial gap motors in general [15].

The discussions that follow are derived from Kaman experience in constructing the prototype and subjective professional opinion regarding projected construction costs of the various motor morphologies considered in this study. They are the author's interpretations of broad generalizations given in support of this work, and are not absolute truths regarding construction practice in general or Kaman procedures in particular. They should not be used as a basis for detailed cost analysis.

Generally, a lead contractor such as Kaman will attempt to subcontract the machine components such that they are delivered in as finished a state as possible. Fabrication and machining of shafts, disks and casings take place at the sub-contractor level, and the cost to the lead contractor for these components is primarily a function of the type and amount of materials involved. The cost of sub-contractor labor, while certainly a factor affecting *actual* cost, does not significantly impact the *relative* cost of a large shaft as compared to that of a similar but smaller shaft, for example. Thus the relative acquisition cost of a motor, up to the point at which its various components arrive at the lead contractor site, may be accounted for by the total *material* cost of the components.

At the lead contractor site, construction takes the form of sub- and final assembly. This assembly involves operations that cannot be done at the sub-contractor level, such as winding the disks, mounting them on the shaft and casing, installing bearings, making electrical connections and incorporating the power electronics components. At this point, the cost of construction becomes less dependent on material volumes than on machine complexity. The primary factors affecting the relative complexity of the machines synthesized in this study are the number of stages and the type of rotor (wound or permanent magnet). If a base construction time is specified for the most simple motor to

construct (permanent magnet rotor, single stage) then the construction time of any other configuration may be approximated by factoring in the relative complexity. The base construction time for a single stage permanent magnet motor is approximately 30 working days. Total labor cost per day for this type of work is approximately $1500, giving a base construction cost (C_{base}) of $45,000. Wound rotor machines should require increased construction time and cost because of the additional windings and connections. Unfortunately, no production history exists on which to base an estimate of the augmenting factor. Subjective analysis of the construction procedures involved for both rotor types and the opinions of industry and academic authorities indicate that a factor of 1.4 is not unreasonable [15], [16]. Construction time would also be expected to increase with the number of stages, although not exactly in proportion. The expected time required for construction of a two-stage motor would not be quite double that for a single-stage, as assembly equipment and personnel will already be in place and operational for the additional work. This redundancy benefit will be somewhat reduced by the alignment procedures required for multiple stages. Again acknowledging that the lack of production data makes any construction cost model an approximation, the model selected for this study based on the previous discussion is shown in Figure 3-1:

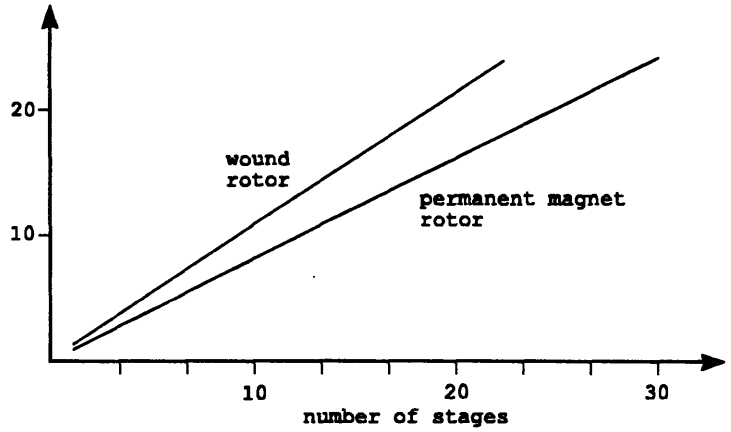

Figure 3-1: Normalized Construction Cost vs. Number of Stages

This function is coded as

$$C_{const} = [0.8n + 0.2] \cdot r_t \cdot C_{base}$$

where the rotor type factor r_t is equal to unity if the rotor is permanent magnet and 1.4 if the rotor is wound.

3.2.5.1.3 Profit Margin

Profit margin is determined by a manufacturer and is normally some percentage of the total cost of materials and construction. It may vary from time to time and among manufacturers, but is normally in the neighborhood of 10% for military contracts. The assignment of this percentage is not completely arbitrary, as it will affect the relative

magnitude of acquisition as compared to life cycle cost, but due to the dominance of life cycle cost in this type of application its effect will in any regard be minimal. The profit margin cost is calculated here as 10% of the sum of material and construction costs. The total acquisition cost is then:

$$C_A = 1.10 \cdot (C_{mat} + C_{const})$$

3.2.5.2 Operational Costs

Navy ships are built to specific operational life cycles. Currently the standard life cycle of a frigate or destroyer type ship is 30 years, although this may be increased to 40 or more years for the next generation of ships. Over periods of this length, the operational costs of a component, which for a propulsion motor include fuel and maintenance costs, will normally be much more significant than acquisition cost.

Operational cost is determined by calculating average annual costs and finding the equivalent in current dollars over the expected lifetime of the motor. This requires the assumption of a discount rate, or prevailing interest rate, for each year of the life cycle. Obviously this rate is not constant and cannot be accurately predicted. In keeping with Navy practice at the time of this writing, the discount rate is taken to be constant at 7% throughout a 30-year motor lifetime. Thus the total lifecycle operational cost, as given by E. P. De Garmo et al., is [17]:

$$C_{OP} = (C_M + C_F)\frac{(1+r)^N - 1}{r(1+r)^N}$$

where C_M is the annual maintenance cost, C_F is the annual fuel cost, r is the discount rate (set to 0.07) and N is the number of years (set to 30). The annual maintenance and fuel costs are discussed further below.

3.2.5.2.1 Maintenance Cost

The average cost of maintenance, although significant, is difficult to predict without some history of usage. However, it is logical to assume that maintenance requirements are at least somewhat proportional to the complexity of the machine. As discussed in the section on construction cost, the two design parameters that most directly affect the complexity of these motors are the number of stages and whether the rotor is wound or permanent magnet. Both of these characteristics are primary design parameters and are easily identified in the motors that will eventually comprise the frontier; that is, if one's intention is to screen motors based on projected maintenance costs, this can be accomplished in a final analysis. This is deemed preferable to attempting the formulation of a subjective algorithm for maintenance and therefore maintenance cost is not evaluated, i.e. it is set to zero in the life cycle formula above for all motors.

3.2.5.2.2 Fuel Cost

The cost of fuel over the ship's lifetime is the most significant of all costs associated with a propulsion motor. Although it would seem to be accounted for by evaluation of the motor's efficiency, the efficiency discussed above is at rated (full power) conditions. A warship spends a small fraction of operational time at full power and since motor efficiency is not proportional to load, the rated efficiency alone is not a sufficient indicator of lifetime fuel cost. A more useful value is the efficiency at the motor's average power output over the ship's life cycle. A study of energy saving techniques for warships by H. C. Schlappi [18] shows that an overwhelming majority of underway time during a typical destroyer mission is spent between 1/3 and 2/3 of maximum speed, with the average speed being slightly greater than half the maximum. Thus a motor attribute of interest to the naval architect is the particular efficiency when power output is such that ship speed is within this range.

Unfortunately, it is incorrect to assume that motor power is proportional to ship's speed and thus to calculate average efficiency. Ship speed is not proportional to power delivered to the propeller nor to propeller rotational speed. This is because the total drag of a ship's hull as it moves through the water is the sum of two independent factors, the friction drag and the wave making resistance. Of the two, wave making resistance is dominant, particularly at higher speeds. While friction drag is a relatively well behaved function of Reynold's number and thus ship speed, wave making resistance is not. It generally increases with speed, but its rate of increase varies and its form as a function of speed is unique to the hull geometry. An arbitrary representation of the relative magnitudes of the two types of drag, characteristic of large ocean vessels, is shown in Figure 3-2.

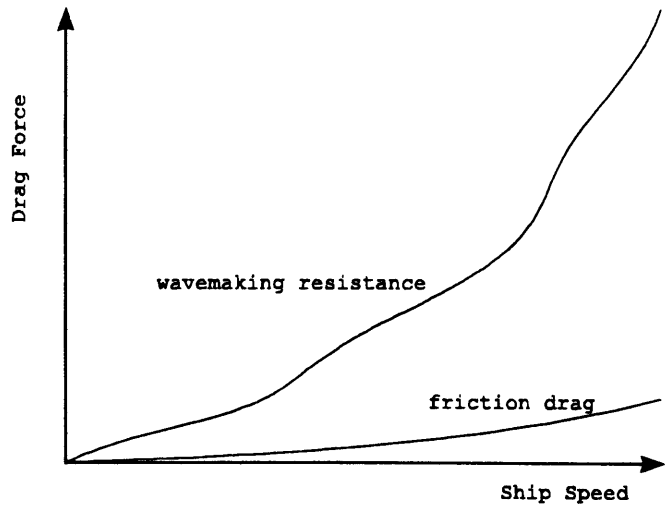

Figure 3-2: Hull Drag vs. Ship Speed

Cancellations between bow and stern waves, among other effects, cause the irregularities in the wave making resistance curve. At present, it is not a calculable function and is generally determined by model testing during the ship design process and updated by full-

scale tests. Therefore, in order to determine total drag at average speed and predict a propulsion motor's corresponding power output, it is necessary to assume a hull form with a history of operation and obtain its powering data. The DD-963 (*Spruance*) class destroyer hull is used here; powering data is given by Schlappi [18]. These ships have a maximum speed of approximately 32 knots. Throughout a typical mission, the average speed is approximately 18 knots, requiring 12,000 shaft horsepower. This is 15% of the 80,000 horsepower installed. Thus if the propulsion system were electric, the motor efficiency to be used in calculating annual fuel usage would be at 15% of rated power, neglecting differences in mechanical and electrical transmission efficiencies. Since synchronous propulsion motors use frequency conversion to change rotational speed, and since the input frequency affects losses, it is also necessary to specify the average rotational speed. For a *Spruance* destroyer the propeller rotational speed is 90 rpm at 18 knots.

Given these values of average lifetime power output and rotational speed, a motor's average efficiency and expected fuel usage may be calculated. In the equations to follow, variables at the average operating condition are indicated by a prime symbol (′); all others are rated values. (Note: *Spruance* class destroyers, as well as *Perry* class frigates and several classes of diesel ships, use a controllable pitch propeller. The average rpm of these ships is not scaleable to ships using fixed pitch propellers.)

The average electrical frequency and the average synchronous reactance are proportional to the mechanical speed:

$$\omega_e' = \omega_e \frac{rpm'}{rpm}$$

$$X_d' = X_d \frac{\omega_e'}{\omega_e}$$

The average power is

$$P' = 3V_a'I_a' \cos(\phi)$$

which is taken here to be 15% of rated power. The power factor angle ϕ is assumed to be constant.

The input power is also a function of the internal voltage, and may be calculated by considering the equivalent circuit for the motor, shown in Figure 3-3.

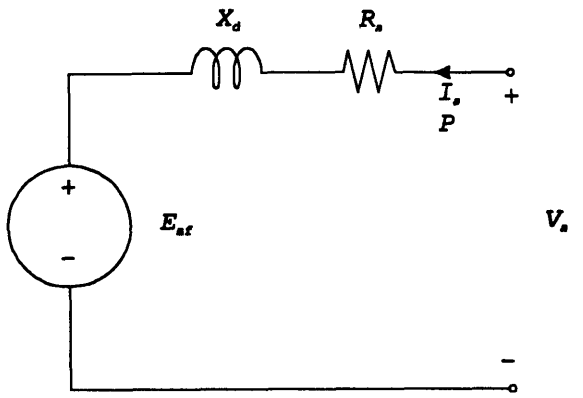

Figure 3-3: Motor Equivalent Circuit

From circuit theory, the real power flow into the circuit at the average operating condition is given by:

$$P' = 3\frac{V_a' E_{af}'}{X_d'} \sin \delta'$$

where δ' is the internal power angle of the motor, or the angle between the terminal and internal voltage phasors. It is shown in the phasor diagram of the motor in Figure 3-4.

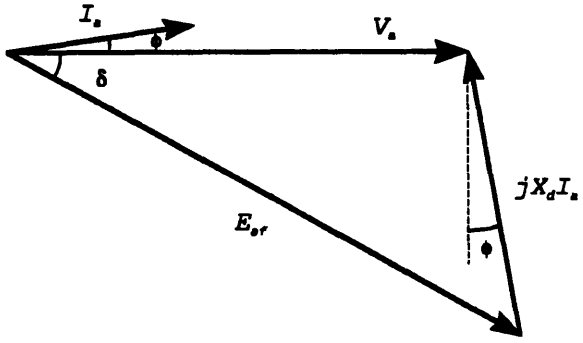

Figure 3-4: Phasor Diagram

The law of cosines gives the magnitude of the internal voltage in terms of the other parameters:

$$E_{af}'^{\,2} = (V_a')^2 + (X_d' I_a')^2 - 2V_a' X_d' I_a' \cos(\phi + 90°)$$

For wound rotors, P', X_d' and ϕ are known and the result is three equations in four unknowns: I_a', V_a', E_{af}' and δ'. Specifying any one of these determines the remaining three and thus the efficiency, as the losses considered in this study are the armature resistance loss (a function of I_a), the field resistance loss (a function of E_{af}) and the core loss (a function of ω_e).

Motor control electronics assumed for this study will have the capability to regulate terminal voltage and current such that the motor operates at the maximum possible efficiency at any rotational speed. This maximum may be found by specifying one of the above unknowns as the independent variable and calculating efficiency as a function of this variable. Armature current is selected as the independent variable here. A representative plot of efficiency vs. per unit armature current, with per-unit terminal voltage overlaid, is shown in Figure 3-5.

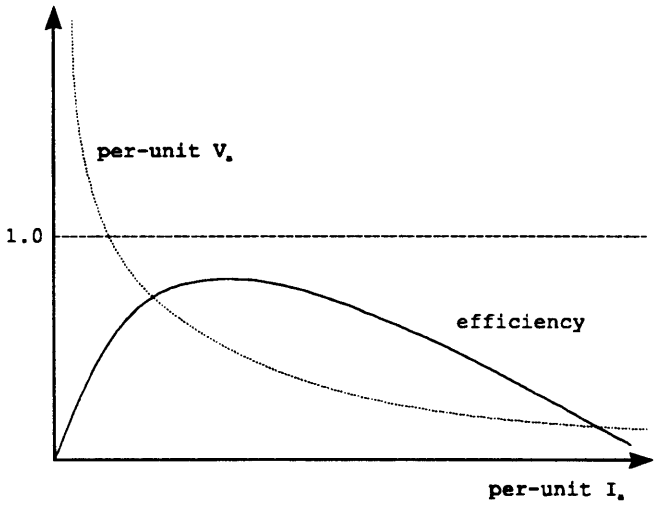

Figure 3-5: Efficiency vs. Armature Current

Efficiency peaks at some value between zero and one per-unit armature current because armature resistance losses increase with armature current, while internal voltage and therefore field resistance losses decrease. Selection of the point at which maximum efficiency occurs is accomplished in the code by specifying a range of armature current at average power and speed, calculating the corresponding efficiencies, and selecting the maximum value. The range of armature current considered is bounded at the high end by its 1 per-unit rated value and at the low end by the value corresponding to 1 per-unit rated terminal voltage.

For permanent magnet motors, E'_{af} is proportional to frequency and is therefore fixed:

$$E'_{af} = E_{af} \frac{\omega'_e}{\omega_e}$$

so that armature current, voltage, power angle and machine efficiency at the average operating point are also fixed. Thus wound rotor machines may be able to realize a much greater *increase* in efficiency at average power as compared to rated power than permanent magnet machines. A wound rotor machine with a capable controller can vary current and voltage at off-rated conditions such that maximum possible efficiency results,

while a permanent magnet machine cannot. Even so, wound rotor machines will generally be less efficient at all conditions because of field losses.

Schlappi assumes 3000 operational hours per year for a destroyer and given the DD-963 machinery configuration of four GE LM-2500 gas turbine engines (two per shaft) and their specific fuel consumption data, calculates average annual ship fuel usage to be 8,312 ltons [18]. Note that this calculation assumes mechanical speed reduction and shafting and includes efficiency factors associated with them. If a 100% efficient propulsion generator and motor were added to this system in series (not a practical arrangement, but useful for analysis), the annual fuel usage would be unchanged. Therefore an indication of a motor's fuel requirements *relative to other motors* may be obtained by inserting it into this system at its average efficiency. Taking the liberty of rounding the above fuel consumption value and assuming one propulsion motor per shaft, the nominal fuel required per year per motor (if the motor's efficiency is 100%) is 4,150 ltons. This nominal fuel weight is divided by the motor's efficiency at average power (η_{avg}), determined above, to give required annual fuel weight. Specifying the price of fuel (c_f) at $200 per lton, a fair value at the time of this writing, gives the annual fuel cost:

$$C_F = \left(\frac{4150\, lton}{\eta_{avg}} \right) \cdot c_f$$

Disregarding maintenance costs, the total cost of a motor over the ship's lifetime is then:

$$C_{TOT} = C_A + C_F \cdot \frac{(1+r)^N - 1}{r(1+r)^N}$$

The optimum value of total cost is considered to be zero.

3.2.6 Robustness

Robustness is a somewhat over-utilized term, and can be taken to indicate any of several propulsion motor attributes. In terms of Navy propulsion, robustness may refer to the ability of the motor to withstand damage. The measure of robustness may be taken to mean the degree to which the motor is degraded after a given amount of damage, the maximum damage the motor can sustain before it becomes totally inoperative, or the maximum damage the motor can sustain before its performance is degraded. In any of these contexts, robustness in military terms is normally referred to as "hardness". Robustness can also mean the inherent resistance of the motor to non-battle factors, such as the corrosive marine environment and the transients inherent in rotating a propeller through a non-uniform (free-surface) medium.

Alternatively, robustness may be defined as the expected failure rate of the component during normal operation, with failure again taken to mean either degradation or total

incapacitation. All of these definitions, as they apply to Navy propulsion, are considered in this section.

The presence of the marine environment is inconsequential in terms of the relative evaluation of these motors, as all are constructed of the same materials. They are assumed to have reasonable protection against chloride intrusion, being located well within the watertight boundaries of the hull and in an environment as controlled as possible and identical for all designs. The type of rotor utilized is not considered significant in evaluating relative robustness as related to the marine environment. In addition, the transients due to speed changes and propeller emergence apply equally to all motors and are not considered to be an influencing factor.

Battle damage effects are certainly of importance. Battle damage can assume many forms; those normally considered in the architecture of warships are shrapnel, shock, flooding and fire. Resistance to shrapnel is a function of a component's outer skin; it is assumed here that any penetrating shrapnel will incapacitate a motor. Thus shrapnel resistance for propulsion motors is determined primarily by the thickness and material of the casing. The casing material for all motors synthesized in this study is identical and therefore not a candidate for evaluation; however, the casing thickness may vary. As discussed in the section on structural design, it is set to the maximum value resulting from three separate stress criteria calculations:

1. The shear stress induced by the total torque of the stator disks (which is constant for all motors, as the power rating and the rated speed are specified).

2. The bending stress resulting from the combined weight of the stator disks.

3. The runout, or maximum displacement of the casing due to the combined weight of the stator disks, expressed as a percentage of the total machine length and limited to 1%.

Trial runs with the design code indicate that very few non-dominated motors that survive maximum length and diameter checks require modification of the casing thickness based on the last two criteria. Practical frontier motors almost universally have a casing thickness based on the stator torque, which is constant. The thickness is therefore very nearly proportional to the disk outer radius. Thus a large motor, which has a greater probability of being hit by shrapnel, has a proportionally thicker case that increases its resistance. Because of this cancellation effect, and also because shrapnel resistance is easily augmented by installing additional plating, shrapnel resistance is not considered to be an attribute for evaluation.

In evaluating a propulsion motor's resistance to shock, the primary factors involved are the motor's natural frequencies and internal clearances (the construction methods and quality are assumed identical for all motors). A motor with relatively low natural frequencies will normally be more susceptible to the impulse created by an internal or

external explosion. Determination of the natural frequencies of motor components is beyond the scope of this thesis; however, it can be said in general that large motors will have lower natural frequencies than small motors and also that as any one physical dimension becomes large relative to the remaining dimensions, the motor becomes more susceptible to shock. For example, a relatively long motor of small radius would be susceptible to "whipping" if its foundation were subjected to a shock impulse, while a short motor of large radius would tend to shudder; either situation would create possible contact between internal components and cause large stresses in foundation mounts. Of course, the installation of additional or improved mounting mechanisms can diminish these effects.

Internal clearances are not modeled in this preliminary design, with the exception of the air gap width which is a variable design parameter. While a large air gap would seem to be preferable in terms of shock resistance, consideration must be given to the fact that all motors are designed to identical power ratings and are limited by a common maximum current density. A wider air gap will require larger, heavier rotors and stators capable of "throwing" flux a greater distance and the result is increased overall size and weight, which as stated above will tend to decrease resistance to shock. In any regard, the range of gap lengths allowed in the design routine is small enough that no measurable differences in shock resistance should exist among motors due to gap length. Thus, based on this elementary analysis, the only motor attributes which have a primary effect on shock resistance are the physical dimensions. Small motors are preferred due to their relatively high natural frequencies, and similar values of diameter and length may be preferable due to the natural resistance of these combinations to deformation. Size is evaluated by the previously considered volume attribute, placing priority on smallness, and therefore does not require an additional evaluation. The relative magnitudes of the overall diameter and length, however, are not yet accounted for.

Resistance to the two remaining forms of damage, fire and flooding, is considered to be identical and non-quantifiable for all motors synthesized and is not evaluated. Thus in this analysis the assessment of a motor's resistance to battle damage is reduced to optimization of total volume and the relative magnitudes of diameter and length. As before, total volume becomes optimum at zero. The desired "squareness" of the motor is evaluated by considering the ratio of length to diameter, where a value of unity is optimum. This very general assertion will be revisited when the impact of length to diameter ratio on shaft angle and arrangeability is discussed in those sections.

In terms of mean time between failure, the relevant characteristics are identical to those of maintenance requirements, namely the number of stages and the type of rotor. As the power rating, maximum current densities and maximum structural stresses of all motors are identical, it is improbable that any other factors will affect the expected failure rate. Although as yet undocumented, it is reasonable to assume that the non-catastrophic electrical failure of one stage of a multi-stage motor would allow continued operation of the motor in a degraded condition. Thus a machine with many stages, while more likely to experience a component failure, will also be more likely to remain operational following a

failure. The advantage of a permanent magnet rotor over a wound rotor in terms of expected failure is in its fewer components and reduced complexity. Thus if the expected mean time between failure is to be evaluated, a large number of stages and a permanent magnet rotor are optimal. These optima are identical to those of the maintenance section and are not evaluated for the same reasons given there.

3.2.7 Shaft Angle

As mentioned in the introduction, the radius of a propulsion motor determines the propeller shaft angle if the motor's location is fixed, or the length of the shaft if the shaft angle is fixed. Normally the shaft angle is constrained by some maximum value (traditionally five to six degrees from horizontal), and the motor must be positioned far enough forward so that this constraint is satisfied. This would seem to indicate that optimum motor radius should be set to zero regardless of the motor's length; however, it must be noted that shaft angles *less* than the constraint will likely produce diminishing returns in terms of propeller efficiency. Also, since the rated power of this type of machine is a function of the square of radial dimension but is only proportional to machine length, machine *volume* increases as the length to diameter ratio increases. Therefore it would be inconsistent to evaluate motors on an absolute radius basis, particularly when the volume attribute is also to be evaluated with its zero optimum. To a large degree then, in terms of shaft angle criteria, any motor that satisfies constraints is as good as any other. As discussed in Section 3.1, this type of situation is best handled by a limit check rather than an attribute evaluation. Limit checks are independent of the attribute evaluation process; the machine radius limit imposed and other limit checks employed are discussed in Section 4.3.

3.2.8 Arrangeability

The arrangement of components within the various spaces of a ship is a series of compromises. The most desirable location of a component is dictated by several factors including proximity to related systems, ease of access and the distance of the location from the ship's center of gravity, as vertical accelerations increase with this distance. It is also desirable to separate redundant systems so as to prevent the loss of two or more in the event of localized battle damage. These are just a few examples; many other factors influence the placement of systems aboard ship and the study of their inter-relationships is quite involved. The net effect is that many components compete for the same space. Coupled with the fact that space is at a premium on a warship due to the pursuit of low overall cost and high payload fraction, the result is a dense distribution of components, particularly in machinery spaces where the volume of human traffic is low. Since machinery will be densely arranged, it follows that the shape of a machinery component has a definite impact on its desirability aboard ship. Oddly shaped components with unwieldy projections or dissimilar length, width and height dimensions would be expected to cause arrangement difficulties. This is generally true; however, since most components will not occupy the total volume between their footprint and the deck above (the overhead), it can reasonably be asserted that deck area is at more of a premium than compartment volume. In this sense, a short motor of large radius would be preferable to a

long motor of small radius, as the latter would require not only more volume per unit power but also more deck area. Of course, the radius is limited by the deck height and the shaft angle criteria mentioned above.

In warships, deck height is normally between 9 and 12 feet, and a considerable amount of this is used for overhead routing of pipes and cables. Continuous decks, and therefore consistent deck heights, are desirable in order to avoid stress concentrations. Objects that exceed the nominal deck height require discontinuous decks and structural modifications to the ship, thereby increasing production costs. Discontinuous decks are usually found in main machinery spaces where large prime movers are located, but are not necessarily required for a propulsion motor room if the motor can be made small enough. Thus the ideal propulsion motor in terms of arrangeability has low volume, is of greater diameter than length and does not exceed the prevailing deck height in non-main machinery spaces. This indicates an optimum volume of zero and a length to diameter ratio *equal to or less than* unity, as long as the motor satisfies maximum radius criteria.

In summary, the three attributes which are affected by motor dimensions indicate that length and diameter should be as nearly equal as possible (robustness), that radius must be at least as small as non-main machinery room deck heights (shaft angle and arrangeability) and that the length to diameter ratio should be between zero and one (arrangeability). The shaft angle criterion is inherently satisfied by the limit check. The robustness criteria are admittedly rather vague, and although it is fortunate that the optimal dimensions arrived at are somewhat consistent with those of arrangeability, they are not considered to have a significant impact on overall desirability. In any regard, they can be fairly well accommodated by applying only the arrangeability criterion, which includes a length to diameter ratio of unity in its optimal range. These arguments would suggest a desirability function based on the length to diameter ratio that is maximum between zero and one and decreases steadily for values greater than one due to the greater deck space and compartment volume required by such motors. The function selected to represent this is shown in Figure 3-6.

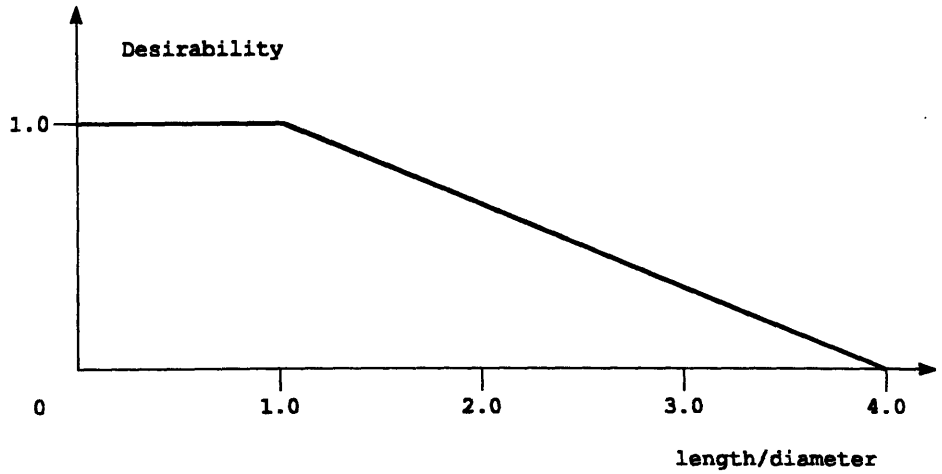

Figure 3-6: Length/Diameter Desirability Function

This desirability function has an optimum value of unity and is calculated using the stack length of the machine and the case outer diameter. Negative values of the function are possible and allowed by the design code.

3.2.9 Noise Level

Noise level is quite difficult to quantify from a preliminary design standpoint. It can reasonably be assumed to depend on numerous characteristics such as the number of stages, the "roughness" of the windings as they rotate in the gap, the mechanical rotational speed, the number of support bearings, etc. The motor can also be expected to generate noise through vibration and flexure of its casing and internal elements at harmonics of the rotational speed. This type of noise is more significant in warships, as it is transmitted to the ship's hull and directly into the water. Resonance conditions and natural frequencies of components will certainly have an impact on the magnitude of this type of noise, as will the makeup of the machine's foundation and any isolation devices installed. The number of factors influencing noise level and the fact that several of them are not quantified in preliminary design puts noise level calculation beyond the scope of this study; it is not considered for evaluation here. However, in general an electrical propulsion system will produce less vibrational noise than a comparable mechanical system due to the absence of mechanical meshing in gears. This benefit may be somewhat reduced if the required cooling system for the motor uses high pressure gas or liquid, which will produce broad band noise.

3.2.10 Reversibility

Reversibility of a marine propulsion system refers to the capability of the system to move the ship astern. For mechanical transmissions, this must be accomplished by either reversing the rotation of the prime mover (possible only with steam turbines), reversing the pitch of the propeller blades (used for gas turbines and diesels) or by some type of auxiliary reversing gear such as that installed on the AOE-6 (*Supply*) class. The ease of reversal and impact of required reversing components influence the desirability of propulsion systems using these types of arrangements. However, since reversibility is inherent in synchronous electric motors by changing the phase sequence and since this capability is assumed in the power electronics, it is not considered for evaluation.

3.2.11 Risk

Risk factors associated with the proposed acquisition and installation of any system account for the likelihood that the system will not meet expectations. Cost risk, for example, is the likelihood that cost overruns will occur in development, production or installation. This is primarily a function of the state of the technology involved in building the system and the experience or lack thereof in adapting it to shipboard use. Other risk factors, such as whether the system will perform as expected over its lifetime and what the required action will be if it does not, are also basically functions of the "newness" of the technology and its application. While all motors designed here can be considered to have

a high risk factor because none have been produced in this power range, the risk involved is consistent among them and is therefore not an attribute of evaluation. The difference in the state of technology between wound and permanent magnet rotor machines is acknowledged, but again this is a primary design parameter and is available for final screening of the frontier.

3.3 Attribute Summary

Of the eleven decision-impacting attributes discussed in this chapter, five (weight, volume, rated efficiency, lifecycle cost and heat density) are determined to be worthy of evaluation on their own merit. Three others (robustness, shaft angle and arrangeability) are in a sense combined to result in a sixth attribute, the length to diameter ratio. The remaining three (noise level, reversibility and risk) are either non-quantifiable or have no relative effect. The following table summarizes the attributes chosen for evaluation and their optima.

Table 3-2: Evaluated Attributes and Optima

Attribute	Optimum
weight	0
volume	0
rated efficiency	100%
lifecycle cost	0
heat density	0
length/diameter	0-1.0

4. Application of the Novice Design Method

Chapters 2 and 3 deal with the independent processes of motor design and attribute evaluation. The Novice method by which these processes are combined for optimization and the type of results which may be expected using this method are discussed in this chapter.

4.1 Attribute Comparison

When attributes have been identified and defined and their optimum values have been determined, the comparison process itself is quite simple. As each new motor exits the design module, each of its six relevant attributes from Table 3-2 are compared individually to those of all motors currently on the frontier (the first feasible motor initiates the frontier). If the new motor dominates any motor on the frontier (again, domination by the new motor means that all of its attributes have values closer to the optima), then the dominated motor is discarded. If the new motor is dominated by any of those on the frontier, the new motor is discarded. If neither of these situations occur, the new motor is added to the frontier.

There are many ways to implement this process in programming. Here, it is accomplished by the use of a summing variable, set to zero prior to each comparison. As the attributes of the new motor and a frontier motor are compared, the summing variable maintains a tally of new motor's attributes which are closer to the optima. A final value of zero indicates that the new motor is dominated by the frontier motor. If the new motor is dominated by a frontier motor, it cannot possibly dominate any other frontier motor. The evaluation process is terminated, the current frontier is preserved and the design code generates the next motor. A summing variable value between zero and six indicates that neither motor dominates the other. The frontier motor is retained and the comparison process moves on to the next frontier motor. A summing variable value of six indicates that the new motor dominates the frontier motor. The frontier motor is discarded and the process moves on to the next frontier motor. If the new motor is not dominated before it has been compared to all frontier motors, it is added to the frontier. The evaluation process is complete when the new motor has either been dominated or has been compared to all existing frontier motors. The design code then generates another motor and the process is repeated.

4.2 Gaussian Mapping

When applying this type of attribute comparison process, it is obviously desirable to generate as few inferior motors as possible. Generation of a motor that is dominated by existing frontier motors contributes no useful information. It would therefore seem logical to concentrate the search for non-dominated designs around a point where a previous

"hit" has occurred. In initial attempts to increase the hit rate, one might be lead to restrict the design parameters to narrow ranges centered at the values of a previous success or possibly to calculate gradients at that point and attempt to "climb the hill". In multi-objective optimization this approach may have unacceptable consequences. It must be remembered that the process itself is necessary because the form of the cost function is unknown. Concentrating the search around a previous hit may constrain the process to the area of a local (and possibly insignificant) maximum. On the other hand, a hit does indicate that a relatively "good" combination of parameters has been found and it would be illogical to completely abandon this area on the premise that there are better areas yet unexplored. Some sort of compromise would seem to be in order.

Several methods of exploring the region of a hit while maintaining the creativity of the Novice method are available. They include the hill climbing technique mentioned above, with some sort of termination criteria applied at the point of diminishing returns. A similar but less computationally intensive technique might involve randomly searching the area of a hit with termination upon a specified number of iterations. Both of these methods have merit. However, if the design routine is simple enough that the processing time per design is acceptably small, it can be argued that the most informative results are obtained by continuing to emphasize the creativity of the search. In other words, if a large enough number of designs can be generated in the processing time available, the designs comprising the frontier will indicate the form of the cost function. In particular, a frontier motor's attributes as compared to optimum values will be indicative of the magnitude of the maximum on which the motor lies. The degree to which this premise is true will increase with the number of non-dominated designs produced. If significant maxima are apparent on the eventual frontier (i.e., if there exist frontier motors with strong values of most or all attributes), the process may be re-initiated with design parameters restricted to those regions in order to further explore the maxima.

The parameter modification process selected here is a Gaussian distribution centered on the parameter values of a previous hit. This preserves the creativity of the method while giving due consideration to a successful combination of parameters. If a newly synthesized motor is dominant, the parameter specification process for the next 20 motors is modified such that the probability density function of each parameter is Gaussian, with mean equal to the previous hit motor's corresponding parameter and a standard deviation equal to 1/30 of the parameter's range from Table 2-1.

From probability theory, it is known that for a normally distributed function the probability that a function value is within one standard deviation of the mean is approximately 68%, the probability that it is within two standard deviations is approximately 95.4%, and for three standard deviations the probability is 99.7% [19]. The normally distributed random number generator in MATLAB™ produces values based on a density function of zero mean and unity standard deviation. Thus there is a 99.7% chance that the number generated is between +3 and -3. Dividing this output by 3 and multiplying by half of a parameter's range makes the probability 99.7% that the number is not removed from zero by more than half of the parameter's range. Further division "squeezes" the density

function around the zero mean. The magnitude of this further division may be varied to give any desired probability density as a function of the parameter's range. For this study, the divisor is selected to be 10, resulting in the standard deviation of 1/30 from above. Finally, the previous successful motor's parameter value is added to the result, effectively shifting the mean of the function. Thus, with 99.7% probability, a parameter generated for a motor following a hit will fall somewhere in a span centered on the hit motor's value and extending in both directions for 5% of the parameter's range.

Since there exists the possibility that a parameter may lie outside its *physically* feasible range given the nature of a normal distribution, each value is checked against these limits and chopped if necessary (see Table 4-1). This prevents, for example, negative disk radius or zero poles. These normal distributions are used for 20 subsequent iterations unless another hit occurs, in which case the counter resets and the new hit motor's parameters are used for the mean values. After 20 iterations without a hit (and prior to the first dominant motor) the probability density functions of all parameters are set to a uniform distribution across the ranges given in Table 2-1.

Table 4-1: Parameter Feasibility Limits

Parameter	Lower Feasible Limit	Upper Feasible Limit
air gap width	1 mm	∞
disk inner radius	0	∞
disk outer radius	inner radius	∞
max stator tooth flux density at inner radius	0	1.9 T
number of rotor/stator pairs	1	∞
number of pole pairs	1	∞
number of wound rotor slots per pole	1	∞
number of stator slots per pole per phase	1	∞
permanent magnet angle subtended	0	180 electrical degrees
wound rotor slot factor at disk inner radius	0	1
wound rotor slot height	0	∞
stator slot fraction at disk inner radius	0	1
stator slot height	0	∞
stator winding pitch	0	1
type of rotor	0	1

4.3 Design Feasibility Checks

While a physically feasible set of design parameters is *necessary* to produce a feasible motor, it is not *sufficient*. Further feasibility checks become possible as the design progresses, and help to reduce processing time by allowing termination of infeasible designs as they are detected. Designs may be considered infeasible due to physical or application-specific requirements. Physical feasibility constraints are somewhat self-evident; examples from this study include the requirements of positive gap length after implementing a permanent magnet rotor and positive shaft outer diameter after calculating

edge turn thickness. Others, such as the limit on slot height discussed in Section 2.3.2, are necessary to preserve the validity of the design algorithms.

Warship-specific feasibility checks used in this study involve the machine overall diameter and stack length. Diameter is limited to four meters to ensure that frontier motors do not exceed nominal deck heights and thus pose arrangement difficulties (see Section 3.2.8). The stack length limit is necessarily subjective; it is set to seven meters here. This is chosen more as a maximum reasonable value than as a limit on compartment length; together these requirements define a liberal upper limit on motor volume and are generally not expected to exclude otherwise feasible designs. A summary of design feasibility constraints used in the code is shown in Table 4-2.

Table 4-2: Design Feasibility Constraints

Parameter	Limit
stack length	≤ 7 m
machine diameter	≤ 4 m
slot height	≤ 3 slot widths
gap length	> 0
shaft inner diameter	> 0, real
shaft outer diameter	> 0

The seemingly redundant shaft inner and outer diameter checks are a result of the fact that the outer diameter check occurs first in the code, after the edge turn thickness is calculated. The synthesis may then be terminated if necessary prior to inner diameter calculations. The real constraint on shaft inner diameter is a result of the 4th order root solver used in the code which may result in infeasible imaginary solutions.

4.4 The Non-Dominated Frontier

When the iterations are complete, some fraction of the total number of physically feasible motors remains, these having not been dominated by any other motor. This is the *n*-dimensional frontier mentioned in Chapter 1. The final number of motors on the frontier is obviously a function of the number synthesized and the limitations imposed by the feasibility checks. It is also, however, a function of the number and type of attributes evaluated. Consider a simplistic case where only one attribute is evaluated: regardless of the number of motors generated there can be only one motor that is better than the rest (disregarding computer round-off). However, when two or more attributes are evaluated, the size of the frontier is limited only by the number of iterations, assuming that at least one of the following is true:

1. *One or more of the attributes are continuous, or*
2. *The number of iterations is less than the number of possible combinations.*

To see this more clearly, assume that this evaluation process is applied to a product that has two relevant attributes, and these are both represented by real numbers between 1 and

10 with 10 being the optimum in both cases. Assume the first product synthesized scores a {10 5} and initiates the frontier. Then a subsequent product scoring a {9 4} is dominated, but one scoring a {9 6} is not. The {9 6} product is added to the frontier, as would be a {8 7}, a {7.5 7.5} or a {9.999 5.001}. Moreover, none of these new products would dominate each other and the frontier size is equal to the number of products generated (or one less than the number generated, if the {9 4} occurred). Note that this example and the discussion to follow assume that all iterations produce feasible designs. In fact, feasible designs comprise a small fraction of the total attempted in this study, but this fraction is nearly constant as the iterations progress. In this example and the following discussions, the phrase "number of iterations" is used for simplicity, where "the number of iterations resulting in feasible motors" would be more precise.

The example above shows that the number of products on the frontier may range from one to the number of iterations; not a particularly useful fact. The *types* of attributes evaluated and the degree to which they are opposing or redundant have a greater impact on the eventual frontier size. Evaluation of opposing attributes will tend to result in a relatively large frontier; evaluation of redundant attributes will tend to result in a relatively small frontier. Consider two of the attributes chosen for evaluation in this study, machine volume and heat density. While low volume does not directly dictate high heat density, there is certainly some correlation between the two. It is unlikely that any frontier candidate will dominate another in both categories; this is an example of two somewhat opposing attributes. The generation of a few "super" motors that dominate all other feasible designs, while certainly a worthy goal, cannot be expected if opposing or semi-opposing attributes are evaluated. Rather, the frontier will generally continue growing with the number of feasible motors generated if absolutely opposing attributes are present or at some decreasing rate if semi-opposing attributes are present.

On the other hand, attributes such as volume and weight are quite compatible in regard to their optimum values; a motor with low weight will probably also have a low volume and vice-versa. This is an example of two somewhat redundant attributes. Dominance of one motor over another in *both* categories should be quite common; this will reduce the number of motors which reach the frontier only because of low weight *or* volume. The result is obviously a smaller frontier.

The attributes evaluated in this study, and those likely to be encountered in any optimization, are a combination of the two types discussed above. Therefore, not only is the actual size of the frontier unpredictable but its "smallness" will not be an indication of the method's success. In general, the frontier cannot be expected to consist of a small set of excellent products. This is partially a result of the fact that no *relative* weightings are assigned to the attributes.

What is left to be determined, then, is the benefit of this potentially very large set of non-dominated designs. Obviously a production candidate cannot be selected at random from the frontier, as a given frontier motor may be very weak in all attributes but one. Sifting through the entire frontier to isolate designs having relatively strong values of all attributes

is not practical or objective. The value of the frontier, then, lies primarily in the statistical analysis it allows, specifically:

1. *One or more design parameters may exist in a normal distribution with a small standard deviation on the frontier.* This would indicate that the parameter has an optimal value for the application considered. However, if this value does not correlate well with frontier distributions of other parameters, it may not be a useful result in itself.

2. *There may be correlation, linear or otherwise, between design parameters and attributes.* This result would allow more focused design methods to result in desired attribute values. Ideally, all attributes would show significant correlation to one or more design parameters. In this case, the optimal design for the application would be evident. If only some attributes correlate, or if different attributes correlate to different parameters, the benefit of this result becomes more obscure.

3. *Optimal motors may be isolated without relative weighting of the attributes.* Regardless of whether any or all of the attributes are normally distributed on the frontier (and they should be, unless their effect on overall desirability is insignificant), their mean values and standard deviations may be calculated. Frontier designs having strong values of all attributes may then be isolated by filtering the frontier based on the attribute means. If frontier designs exist for which *all* attributes are better than their *frontier* mean values, some measure of success is indicated in that these designs are not only non-dominated, but are also "better" in all respects than the average non-dominated design. If designs exist for which all attributes are better than their frontier means by some non-zero percentage of their standard deviations, the degree of success increases. A reasonable goal in this type of analysis would be the isolation of a frontier design that is better than the frontier mean by a full standard deviation of all attributes. Whether and to what degree this is possible depends on the opposing or redundant nature of the attributes. Also, use of the method itself may be limited by the size of the frontier. It would be inadvisable to base decisions on the means and standard deviations of a small data set.

4. *If necessary, subjective weighting of attributes may be applied to designs on the frontier to isolate the most desirable.* Even when obvious differences in relative importance exist among the attributes, applying the decision tree method discussed in Section 1.2 *after* all dominated designs have been excluded decreases the size of the solution set, perhaps drastically. If the iterations have been continued to the point where the frontier rate of growth is very small or zero, it will be relatively certain that no potentially high-scoring possibilities have been overlooked. Also, the frontier itself will provide useful input to the weighting process based on the attribute distributions.

5. Results

This chapter details the results of 8,350,000 iterations of the design and evaluation process. These iterations resulted in 363,050 feasible motors, of which 1,457 were non-dominated.

5.1 Frontier Size

There are roughly 1.3×10^{13} possible combinations of parameters, given their ranges and increments as specified in Table 2-1 (this value does not take into account the normal distributions invoked following a dominant motor or the fact that the lower limit on disk outer radius is dependent on the inner radius). The fraction of iterations resulting in feasible designs was nearly constant at 0.043 throughout the procedure. If this fraction is considered representative of the entire solution space, there are about 5.6×10^{11} feasible combinations possible. Since 363,050 of these were formulated and evaluated, the ratio of data obtained to the total possibilities is 6.5×10^{-7}. The use of such a small sample on which to base conclusions is certainly questionable. However, two critical factors indicate that this data is in fact representative of the entire solution space. First and most prominent is the fact that the number of non-dominated motors as a fraction of the feasible motors produced decreased steadily and was quite small at the end (see Table 5-1). If the solution space had been inadequately sampled, the frontier should have continued growing at some constant or near constant rate. Second, the design parameters were present in nearly normal distributions among the motors on the frontier. Normal distributions would be improbable if the solution space had been inadequately sampled.

Note the lack of any substantial *decrease* in frontier size as the synthesis progressed, as would occur if any single motor exiting the design module were dominant over multiple frontier motors. This confirms the expectations of Section 4.4. The semi-opposing nature of the attributes made it uncommon for any motor to be totally dominant over another and highly unlikely that multiple motors will be dominated. From the final count of 1,475 non-dominated motors, it is obvious that this method did not result in a small set of "very good" motors from which to select a production model.

The slope of the curve in Figure 5-1 is the rate of increase of the frontier size as a function of the number of feasible motors generated. Table 5-1 summarizes this rate of increase at various points during the synthesis.

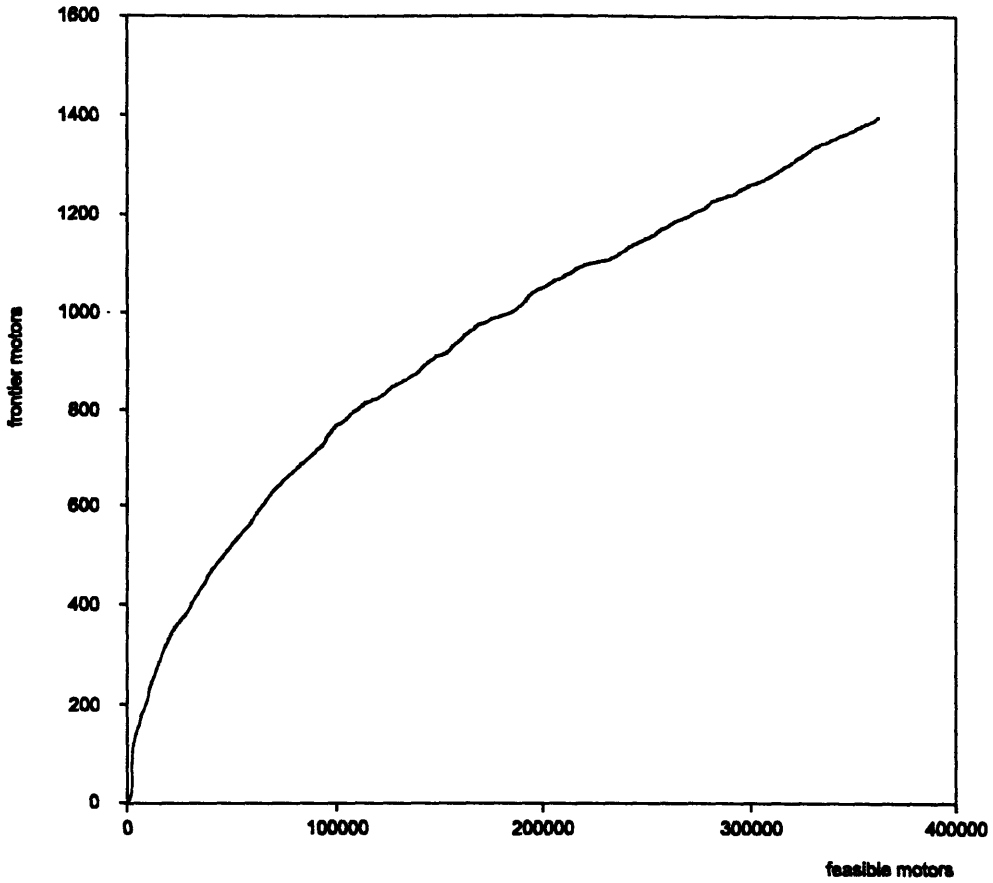

Figure 5-1: Frontier Size

Table 5-1: Frontier Rate of Increase

Feasible Motors Generated	Frontier Increase per Feasible Motor
1	~1
50,000	~0.0051
100,000	~0.0040
150,000	~0.0027
200,000	~0.0024
250,000	~0.0021
300,000	~0.0019
350,000	~0.0018

The steadily diminishing rate of increase suggests that the frontier size is a logarithmic function of the number of feasible motors generated. A simple method of approximating the total number of non-dominated motors which exist in the solution space is to plot the logarithms of the frontier size vs. feasible motors and extend any linear trends through the total number of feasible motors as approximated above. This type of plot for the data obtained is shown in Figure 5-2.

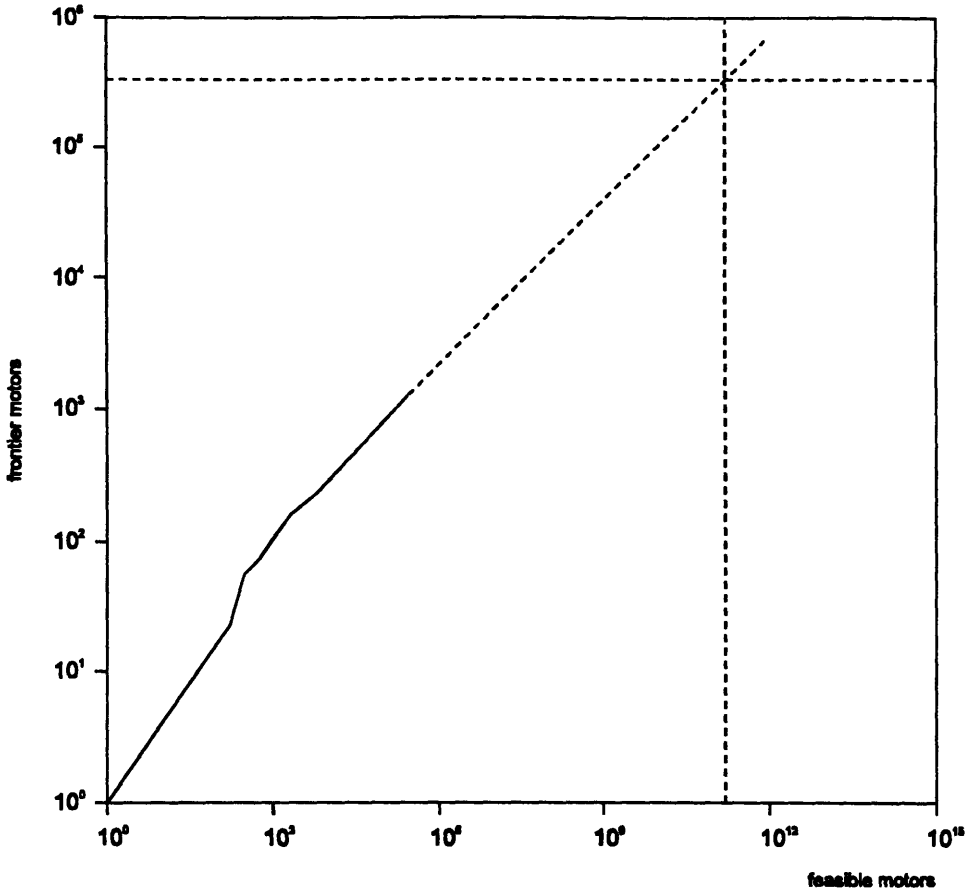

Figure 5-2: Frontier Size Limit

Extending the linear trend of the process through the approximated number of feasible motors in the solution space (5.6×10^{11}) gives an upper limit of approximately 200,000 non-dominated motors. This would indicate that the 1,475 non-dominated motors on the frontier are 0.7% of those which would be found if all possible combinations were evaluated. This small sample may be considered representative of all non-dominated motors only if the solution space has been evenly sampled (of which there is little doubt) and if the sampling is dense enough that local maxima cannot exist between samples. The latter premise is somewhat validated in Section 5.5, where methods of isolating the most desirable frontier designs are discussed.

5.2 Frontier Parameter Ranges

As discussed in Chapter 4, one of the useful results of this method is a determination of the ranges to which design parameters are restricted on the non-dominated frontier, particularly if these ranges are normally distributed with small standard deviations. The following table provides a summary of the design parameters and how they were represented on the frontier in terms of their mean values (μ) and standard deviations as a percentage of design range (σ).

Table 5-2: Summary of Frontier Parameters

Parameter	Design Range	μ	σ
disk inner radius	0.50-1.80 m	1.30	0.18
disk outer radius	inner radius-2.0 m	1.87	0.06
stator slots/pole-phase	1-3	1.17	0.15
stator slot fraction	0.2-0.8	0.42	0.16
stator pitch	0.7-1.0	0.85	0.35
stator slot height	1-11 cm	5.00	0.22
magnet span	90-180 elec. degrees	144	0.29
pole pairs	1-40	22.37	0.12
gap length	1-11 mm	2.80	0.12
stages	1-30	17.18	0.24
peak tooth flux density	1.0-1.9 T	1.81	0.14
rotor type	wound, PM	0.997	0.05

Of note are the parameters represented on the frontier with a small standard deviation relative to their design range, as these might be said to have an optimal value (the mean) for this application. Unfortunately, some of the small deviations above were actually a result of limitations or approximations used in the design code. Gap lengths and peak flux densities tended to be constricted by their feasible limits; the majority of frontier motors had small gaps and near maximum flux densities for obvious reasons. Similarly, the number of stator slots per pole-phase was optimal at the minimum. This is not surprising considering that the benefit of multiple slots is reduction of harmonic reactances, which were not calculated. The tight distribution of disk radius is attributable to the fact that it is constrained above and below by the maximum machine radius limit and the outer radius of the shaft respectively.

Of the remaining parameters, only the number of poles, the rotor type and the stator slot fraction had deviations less than 20% of their range. The implications of the rotor type distribution are covered separately in the next section. The small standard deviations of the number of poles and stator slot fraction, which unlike the parameters discussed above would not seem to be affected by any external constraints in the code, are particularly interesting. The effect of slot fraction on motor performance is relatively undocumented, but the results indicate that its effect on the attributes considered for this application is substantial. Based on its highly normal distribution and small deviation, it is not unreasonable to suggest that it is optimal at its mean value of 0.42, at least when the motor is to be used for warship propulsion. Similar reasoning holds for the number of poles, having a mean value of 22.

Histograms of all design parameters and attributes as they existed in motors on the frontier are contained in Appendices C and D. The intermediate values present in the histograms of stator slot height and magnet span are a result of the normal distributions invoked following a dominant motor.

5.3 Wound Rotor vs. Permanent Magnet

Frontier motors were almost exclusively of the permanent magnet rotor type; only four wound rotor designs were non-dominated. This is of considerable note, as approximately 181,500 feasible wound rotor designs (50% of the total feasible designs) were evaluated during the process. As each motor has six attribute values, there were over one million wound machine attributes evaluated. Of these, only 24 were better than *any* of the 8,826 permanent magnet attribute values which eventually comprised the frontier. This indicates an inherent advantage in the use of permanent magnet over wound machines for this application. Furthermore, since five of the six attributes selected for evaluation (weight, volume, rated efficiency, lifecycle cost and heat density) can be considered relevant for any intended use of an electric motor, these results show that permanent magnet machines may be inherently superior for all applications.

5.4 Parameter and Attribute Correlation

The correlation coefficient between two sets of data is a measure of the strength of the linear relationship existing between them. If the data is in two vectors x and y, the correlation coefficient as given by D. L. Harnett is [20]:

$$\rho = \frac{E[(x-\mu_x)(y-\mu_y)]}{\sigma_x \sigma_y}$$

where E denotes expected value, μ is the mean value, and σ is the standard deviation. The correlation coefficient is perhaps more easily described in terms of its square, the *coefficient of determination* (ρ^2). The coefficient of determination is the proportion of total variation in the dependent variable that may be explained by the linear regression curve; in other words, it is a measure of the quality of the regression fit. This type of calculation is used to determine whether causal relationships exist among design parameters and attributes. A correlation coefficient of +1 indicates perfect positive linear dependency between x and y; as one increases the other increases proportionally. A coefficient of -1 indicates perfect negative linear dependency; the relationship is inversely proportional. A coefficient of zero indicates that no *linear* relationship exists.

Table 5-3 summarizes the correlation coefficients between the design parameters and attributes for all non-dominated motors. Highlighted cells in the table indicate correlations of magnitude greater than 0.5, which in elementary analysis is considered the threshold for concluding some causal relationship. Parameters which pertain only to wound rotor machines, such as rotor slot height and rotor slot fraction, are omitted from the table as wound rotors comprised only 0.3% of the frontier. The claim of Section 3.2.7 that increasing the length to diameter ratio of axial gap machines results in greater volume is verified by the correlation coefficient of -0.82 between them (recall that the length to diameter value is a desirability function and not the ratio itself; the function value

decreases as length increases). No other correlations among parameters and attributes are particularly noteworthy.

Table 5-3: Parameter and Attribute Correlation Coefficients

	weight	volume	heat density	lifecycle cost	rated efficiency	length/ diameter
disk inner radius	-0.29	0.11	-0.07	0.17	-0.13	-0.02
disk outer radius	0.13	0.17	-0.18	-0.01	0.19	0.01
stator slots/pole-phase	-0.21	-0.22	0.24	0.05	-0.27	0.16
stator slot fraction	0.38	0.16	0.00	-0.09	0.11	-0.16
stator pitch	0.02	-0.09	0.04	0.00	0.06	0.06
stator slot height	0.64	0.61	-0.41	-0.19	0.38	-0.50
magnet span	-0.41	-0.26	0.19	0.10	-0.18	0.21
pole pairs	-0.44	-0.26	0.16	0.12	-0.17	0.21
gap length	0.17	0.22	-0.14	0.06	0.03	-0.17
stages	0.45	0.60	-0.56	1.00	0.42	-0.45
peak tooth flux density	-0.11	-0.07	-0.05	0.00	0.11	0.06
weight	-	0.89	-0.65	0.45	0.62	-0.75
volume	-	-	-0.72	0.60	0.60	-0.82
heat density	-	-	-	-0.56	-0.84	0.41
lifecycle cost	-	-	-	-	0.40	-0.44
rated efficiency	-	-	-	-	-	-0.41
length/diameter ratio	-	-	-	-	-	-

Granting the possibility that non-linear relationships might exist, all parameter versus parameter and parameter versus attribute plots were also examined for any evidence of non-linear correlation. No further relationships were apparent.

5.5 The "Best" Motor

Using the method described in Section 4.4, one motor was isolated from the non-dominated frontier as having attribute values which surpassed mean frontier values by the greatest percentage of their standard deviations. It is interesting to note that only 127 motors out of the 1,475 on the frontier had mean or better values of all attributes. These were further screened by incrementally increasing the percent of standard deviation by which all attributes were required to exceed their means. The final motor to survive the screening process surpassed frontier means by 40.9% of standard deviations. Its relevant characteristics are shown in Table 5-4. The fact that the "best" motor's attributes exceed frontier means by less than half a standard deviation might be considered less than a complete success; however, this was somewhat expected due to the nature of the attributes as discussed in Section 4.4. Also, it further substantiates the assumption that no steep isolated maxima exist between the sampling points in the solution space. If such maxima did exist, it would be reasonable to assume that at least one would have been

found by the random search and the motor residing on it would exceed frontier means by a more substantial fraction of standard deviations.

Table 5-4: "Best" Motor Parameters and Attributes

General
rated power: 29.8 MW (40,000 hp)
rated torque: 1.69E6 N-m
rated rotational speed: 168 rpm
power factor angle: 5° lagging
stages: 13
pole pairs: 27
gap length: 2.04 mm
peak tooth flux density: 1.7 T
e_{af}: 1.25
rated efficiency: 0.988
average efficiency: 0.998

Rated Losses
stator resistance loss: 2.96e5 W
hysteresis loss: 5.51e4 W
heat density: 1.25e4 W/m^3

Rated Reactance
Leakage reactance: 5.43e-6 ohms/turn^2
Air gap reactance: 1.50e-5 ohms/turn^2
x_d: 0.672

Cost
acquisition cost†: $524,740
lifecycle cost†: $10.84M

Physical
disk inner radius: 1.4 m
disk outer radius: 1.91 m
stack length: 2.26 m
machine outer diameter: 3.92 m
volume: 27.3 m^3
weight: 1.10e5 kg
shaft inner diameter: 2.69 m
shaft outer diameter: 2.70 m

Stator
terminal voltage: 20.37 volts/turn
armature current: 4.90e5 amp-turns
electrical loading: 1.29e5 amp-turns/m
conductor current: 3.6e6 amp-turns/m^2
slots/pole-phase: 1
slot fraction: 0.40
pitch: 0.8
slot height: 5.1 cm
slot width: 2.2 cm
slot packing factor: 0.7
winding factor: 0.95

Rotor
rotor type: TmReB permanent magnet
magnet span: 170 elec deg
magnet thickness: 2.25 mm

† approximated values, not including power electronics

This motor is presented not as the exclusive solution to the optimization of axial gap motors for warship propulsion, but simply as the results of a particular method of screening the non-dominated frontier. There are certainly other methods available for selecting a single design from the frontier. Matrix manipulation software such as MATLAB™ can easily isolate the frontier design having the most optimal value of any particular attribute, the best average value of two or more attributes, etc. Median attribute values rather than mean values may be determined, and the frontier screened based on the percentage by which attributes are better than medians. When such a method is applied to the frontier obtained in this study, the motors surviving the process are nearly identical to those obtained using the mean and standard deviation method.

Alternatively, if there are obvious differences in the relative importance of the attributes, a decision tree method may be implemented. Applying such a procedure after the frontier is constructed allows relative certainty that only the most viable candidates are considered.

The decision tree method requires weighting of the attributes in terms of their relative importance; once this is done it is a simple matter to calculate the highest scoring motor from among those on the frontier. The determination of these weights is a field of study in itself and there are many reasonable approaches. One method which is potentially useful for this frontier is based on attribute ranges. If some attributes exist on the frontier in a much wider range than others, the ranges as percentages of optimal values may be used as a basis for weightings. For example, the rated efficiencies of all frontier motors in this study were concentrated within about 5% of the optimum (see Appendix D). Machine volume, on the other hand, varied nearly 900% between its minimum and maximum values on the frontier. If attribute weightings were assigned corresponding to these ranges, volume becomes 180 times more important than efficiency. The highest scoring motor would then have a relatively low efficiency, but still within 5% of optimum. Volume, however, would be much lower than that of a motor selected using the standard deviation approach above. In a sense, the "payoff" in volume is much greater than the small amount of efficiency sacrificed. Methods such as this, based on frontier attribute distributions, are preferable to the more subjective approach discussed in Section 1.2 when weightings are necessary.

6. Conclusions and Recommendations

The results of Chapter 5 indicate that permanent magnet machines are inherently and significantly more suited to the application of warship propulsion than wound rotor machines. While the degree to which they exceed wound rotor machines in terms of desirability is remarkable, in retrospect the attributes selected for evaluation do tend to favor permanent magnets. Weight and volume are obviously reduced when rotor windings are replaced by magnets. Rated efficiency benefits from the elimination of field resistance losses. The lower acquisition cost of copper windings as compared to magnet material is overwhelmed by the increased lifecycle cost resulting from the field losses at average operating conditions. Heat density is obviously lower when field losses are absent. The length to diameter ratio, considered optimal at values less than or equal to unity, favors permanent magnet machines due to the absence of rotor slots and the resulting reduced stack length.

It is difficult to identify any particular drawbacks to permanent magnet machines, with one exception. If a marine propulsion motor experiences a fault, the windmill effect of the propeller will continue to turn the motor until the shaft is stopped by mechanical braking or the ship's forward speed drops to nearly zero. For wound rotor machines, this does not present a significant problem assuming circuit breakers function properly. A permanent magnet motor, however, will act as a generator and develop power in this situation, as the magnetic field cannot be "turned off". Depending on the nature of the fault, this generated power may be sufficient to cause further, possibly extreme damage to the motor before rotation stops. This situation has been investigated by F. R. Colberg for flux-concentrating motors [21]. His conclusions, based on a 40,000 hp motor experiencing a fault at rated conditions, indicate that approximately two to three megawatts may be dissipated within the motor after it is electrically isolated. This internal power dissipation may be reduced by a factor of approximately 0.2 by physically shorting the motor windings upon isolation. Regardless, significant damage is possible and some method of preventing this situation (such as automatic mechanical braking) is necessary if permanent magnet motors are to be used for marine propulsion.

The isolation of the most useful motors from among those on the frontier using attribute means and standard deviations is a promising technique. While it might seem reasonable to argue that this is merely one particular assignment of weights (in that they are all equal), this approach actually goes beyond any weighting system whatsoever. A true equal weighting scheme would select as optimal the frontier motor with the best *average* of *all* attribute values, and would in fact be subject to the argument above. In contrast, the method used here is dependent upon the distributions of attributes. It is reasonable to expect that a motor having "good" values of all attributes would be acceptable to the customer. Evaluating a representative sample of all possible designs that meet requirements (the set of feasible motors) allows quantification of "good," since the mean attribute values of essentially all non-dominated designs are known. Then if a motor

having all attribute values equal to their frontier mean is *acceptable*, a motor having all attributes better than their means by some percent of their standard deviation is obviously better. The method used here simply extends this reasoning until a single motor survives the screening process.

There are methods available for checking the progress of the design and evaluation cycle which were not implemented in this study. Some of these may allow a better estimate of how well the frontier represents the solution space. In particular, the number of existing frontier designs which become dominated and are therefore eliminated during the evaluation cycle may be tracked as a fraction of the feasible designs generated. A fully formed frontier should have no possibility of domination by any new design; therefore this fraction should approach zero when the frontier is complete. Another value of interest would be the degree to which motors exiting the design cycle are dominated by frontier motors. For example, rather than simply discarding a motor that is dominated, the differences in design attributes may be retained during the evaluation process discussed in Section 4.1. These differences may be summed when the comparison process between two motors is complete, giving an indication of the degree to which a design is dominant over or dominated by another. Tracking the average of such a value as the iterations progress will indicate how "tight" the frontier is becoming.

The correlation coefficients of Section 5.4 provided little new information. Causal relationships among parameters and attributes for frontier motors were either non-existent or obvious. A potential area for further study is a comparison between the coefficients of Table 5-3 and those corresponding to all feasible designs generated. If a particular correlation coefficient is significantly stronger for frontier designs than for feasible designs in general, the assertion that optimal parameter values exist for the application is strengthened.

The macro developed for this study, utilizing fifteen design parameters and six attributes, required approximately 60 hours to complete 8,350,000 iterations on a 33 MHz 486 processor machine. The most time-intensive aspect of the process seems to be the evaluation cycle, particularly as the frontier size becomes large. Processing time reached one hour per hundred thousand iterations near the end of the procedure when the frontier was large. If more parameters or attributes were included, or if the attributes had been of a more opposing nature, the frontier size would have increased more rapidly and processing time would have been considerably greater. In any regard, since it is desirable to evaluate as much of the solution space as possible, the use of this method for other purposes may require a compiled code.

Although this study has shown both the merit of the Novice method for general optimization and the benefit of permanent magnet over wound rotor machines in warship propulsion, only preliminary designs were considered. In an actual decision making process, the code should be expanded to result in detailed designs, taking into account the actual winding connections, second order reactances and losses, and structural elements such as bearings and slot depressions.

Heat densities of most frontier motors, including the motor isolated in Section 5.5, are large enough that current practical cooling methods are inadequate. The cooling problem remains to be resolved if electric propulsion is to be implemented in warships.

Appendix A: Constants and Resident Variables

Parameter	Value
annual discount rate	7 %
assembly labor cost	$1500 /day
bulk copper cost	$2.20 /kg
bulk electrical steel cost	$1.15 /kg
bulk insulator cost	$9.00 /kg
bulk structural steel cost	$0.90 /kg
conductivity of copper	5.9E7 mho/m
manufacturer's profit margin	10 %
marine diesel fuel cost	$200 /lton
mass density of copper	8900 kg/m^3
mass density of electrical steel	7800 kg/m^3
mass density of magnet material	7450 kg/m^3
mass density of structural steel	7800 kg/m^3
mass density of winding insulator	1000 kg/m^3
maximum conductor current density	1E7 A/m^2
maximum shaft runout	1 %
maximum structural steel stress	100E6 Pa
permanent magnet cost	$130 /kg
permeability of free space	1.257E-6 H/m
power factor angle	5° lagging
rated mechanical rotational speed	168 rev/min
rated power	40,000 hp
residual flux density of permanent magnet	1.29 T
saturation flux density of steel	1.9 T
ship service life	30 years
stator slot packing factor	0.7
wound rotor slot packing factor	0.8
Young's modulus for steel	200E9 Pa

Appendix B: MATLAB™ Macro

```
%*************************************************************************************************
%                              Axial Gap Motor Design and Evaluation                              *
%                                     for Naval Propulsion                                        *
%                                                                                                 *
%                                  copyright  Mark W. Thomas 1996                                 *
%                                      all rights reserved                                        *
%*************************************************************************************************

clear
total=400000;
clockstart=clock;

%**************************Resident variables*****************************************************

condCu  =5.9E7;         % conductivity of copper (mho/m);
rhoCu   =8900;          % copper density (kg/m^3)
mu      =1.257E-6;      % permeability of free space (H/m);
Bsat    =1.9;           % maximum flux density in electrical steel (T)
Es      =200E9;         % Young's modulus for steel (Pa)

%**************************Input*****************************************************************

pwr     =40000;         % rated power (hp)
pfang   =5;             % power factor angle (degrees lagging)
RPM     =168;           % rated mechanical rotational speed (rpm)
codmax  =4;             % maximum machine diameter (m)
slmax   =7;             % maximum stack length (m)
hmax    =3;             % maximum slot height (multiples of slot width)
Br      =1.29;          % permanent magnet residual flux density (T)
rhoPM   =7450;          % permanent magnet mass density (kg/m^3)
rhoss   =7800;          % structural steel mass density (kg/m^3)
rhoes   =7800;          % electrical steel mass density (kg/m^3)
rhoins  =1000;          % winding insulation mass density (kg/m^3)
taumax  =100E6;         % maximum structural steel stress (Pa);
packfacs=0.7;           % stator slot packing factor (copper volume/slot volume)
packfacr=0.8;           % rotor slot packing factor (copper volume/slot volume)
Jmax    =1E7;           % maximum copper current density (A/m^2)
sromax  =0.01;          % maximum shaft runout (fraction of shaft length)
N       =30;            % ship service life (years)
r       =0.07;          % annual discount rate
CCu     =2.20;          % bulk copper cost ($/kg)
Cesteel =1.15;          % bulk electrical steel cost ($/kg)
Cssteel =0.90;          % bulk structural steel cost ($/kg)
Cins    =9.0;           % bulk insulation cost ($/kg)
CPM     =143.3;         % shaped permanent magnet cost ($/kg)
daybase =30;            % base machine assembly time (1 stage, wound rotor) (days)
labday  =1500;          % assembly labor cost per day ($)
confacw =1.4;           % construction time augmenting factor for wound rotor machine
pmarg   =10;            % manufacturer's profit margin (%)
Cfuel   =200;           % marine diesel fuel cost ($/lton)
wtfuel  =4150;          % fuel used per 100% efficient motor per year (ltons)
pctpwr  =15;            % ship lifetime average shaft power (% of rated power)
avgRPM  =90;            % ship lifetime average shaft RPM

%*************************************************************************************************

pwr     =pwr*745.7;                             % convert to watts
pfang   =pfang*0.01745;                         % convert to radians
disfac  =((1+r)^N-1)/(r*(1+r)^N);               % discount factor

f4=0;           % parameter probability density flag (0=uniform, 1=Gaussian)
                % set to uniform for first motor

f6=0;           % f6 is increased by one each time a physically feasible
                % motor is generated.  f6=1 initiates the frontier.

f7=0;           % set to 1 if a PM motor fails gap length feasibility.
                % The next motor is forced to PM to balance the iterations
                % between wound and PM rotors.
```

```
f8=0;          % set to 1 if a wound rotor machine fails rotor slot height
               % feasibility.  The next motor is forced to wound.

seed=clock;    % seed random generator to seconds value of system clock
rand('seed',seed(6)*1e4);

runsize(1)=1;  % vector variable for tracking the size of the frontier
               % as a function of the number of feasible motors generated

ans1=input('Continue with the previous frontier (y/n)?     ','s');  % This allows results
                                                                    % to be appended to a
                                                                    % previous frontier
if ans1=='y'
  load base
elseif ans1=='n'
else
  axial
end


for k=1:total          % main loop counter (number of motors to be generated)

  if f4 == 1           % if Gaussian distribution is in effect,
    if k > 20+f5       % if 20 iterations have passed since hit
      f4=0;            % reset parameter distribution to uniform
    end
  end

%******************Generate random design parameters*********************************************

  if f4 == 0           % This section generates the random design
                       % parameters using a uniform probability density
                       % between each parameter's lower and upper limits.
                       % It is used for the first motor generated and
                       % whenever a dominant motor has not been generated
                       % in the previous 20 iterations.

    rand('uniform');                          % set random generator to uniform density
    var =rand(1,15);                          % random number vector
    Ri=ceil(var(1)*1.3*10)/10+0.5;            % disk inner radius (0.5 thru 1.8m, 10 cm steps)
    qs=ceil(var(2)*3);                        % stator slots/pole-phase (1 thru 3 integer)
    lamsi=ceil(var(3)*0.6*10)/10+0.2;         % stator slot fraction (0.2 thru 0.8, 0.1 steps)
    pitch=ceil(var(4)*0.3*10)/10+0.7;         % stator pitch (0.7 thru 1, 0.1 steps)
    p=ceil(var(5)*40);                        % number of pole pairs (1 thru 40 integer)
    Ro=ceil((var(6)*...       % disk outer radius (Ri+1cm thru codmax/2 m, 10 cm steps)
    (codmax/2-Ri)*10))/10+Ri+0.01;
    qr=ceil(var(7)*9);                        % rotor slots/pole (1 thru 9 integer)
    lamri=ceil(var(8)*0.6*10)/10+0.2;         % rotor slot fraction (0.2 thru 0.8, 0.1 steps)
    n=ceil(var(9)*30);                        % number of stages (1 thru 30 integer)
    g=ceil(var(10)*.01*1000)/1000+0.001;      % gap length (1 thru 11 mm, 1 mm steps)
    M=round(var(11));                         % rotor type indicator (0=wound rotor, 1=PM)
    Bti=ceil(var(12)*0.9*10)/10+1;            % peak B in tooth at Ri (1.0 thru 1.9T, 0.1T steps)
    beta=floor((var(13)/2+0.5)*10*pi/p)/10;   % rotor magnet span (90-180 deg, 0.1 rad steps)
    hss=ceil(var(14)*0.1*100)/100+0.01;       % stator slot depth (1 thru 11 cm, 1 cm steps)
    hsr=ceil(var(15)*0.1*100)/100+0.01;       % rotor slot depth (1 thru 11 cm, 1 cm steps)

  else                 % This section generates the random design
                       % parameters based on a normal (Gaussian)
                       % distribution.  For each parameter, the standard
                       % deviation is 3.33% of the range from the uniform
                       % distributions and the mean is the parameter value
                       % from the last dominant motor.
                       % Parameters which are not within feasible
                       % physical limits are chopped.

    checkall=0;        % flag (set to 1 if any parameter is not within physically feasible limits)


    rand('normal');          % Note:  rand('normal') is obsolete in later
                             % versions of MATLAB.  Use var=randn(1,15).

    var=rand(1,15);                                   % random number vector
    Ri=ceil((var(1)*(1.3/6)*0.1+Rih)*10)/10;          % disk inner radius
    qs=ceil(var(2)*(2/6)*0.1)+qsh;                    % stator slots/pole-phase
```

```
  lamsi=ceil(((var(3)*(0.6/6)*0.1)+lamsih)*10)/10;        % stator slot fraction at Ri
  pitch=ceil(((var(4)*(0.3/6)*0.1)+pitchh)*10)/10;        % stator pitch
  p=ceil(var(5)*(39/6)*0.1)+ph;                           % number of pole pairs

  if p < 1                                                % prevent # poles <= 0 for beta calc
    p=1;
  end

  Ro=ceil((var(6)*(1/6)*0.1+Roh)*10)/10;                  % disk outer radius

  if Ro <= Ri                                             % prevent Ro <= Ri
    Ro=Ri+0.01*Ri;
  end

  qr=ceil(var(7)*(8/6)*0.1)+qrh;                          % rotor slots/pole
  lamri=ceil(((var(8)*(0.6/6)*0.1)+lamrih)*10)/10;        % rotor slot fraction at Ri
  n=ceil(var(9)*(29/6)*0.1)+nh;                           % number of stages
  g=ceil(((var(10)*(.01/6)*0.1)+gh)*1000)/1000;           % gap length
  M=Mh;                                                   % retain rotor type after hit
  Bti=ceil((var(12)*(0.9/6)*0.1+Btih)*10)/10;             % peak flux density in tooth at Ri
  beta=floor((((var(13)*(.5/6)*0.1)*pi/p)+betah)*10)/10;  % span of a rotor magnet
  hss=ceil((var(14)*(0.1/6)*0.1+hssh)*100)/100;           % stator slot height
  hsr=ceil((var(15)*(0.1/6)*0.1+hsrh)*100)/100;           % rotor slot height

  %********Chop parameters to upper or lower physically feasible limit if necessary************

  varn=[Ri,qs,lamsi,pitch,p,Ro,qr,lamri,n,g,M,Bti,beta,hss,hsr];

        %Ri  qs lamsi pitch p  Ro  qr lamri n    g   M  Bti beta  hss  hsr
  lower=[ 0,  1,  0,    0,  1, Ri,  1,  0,  1, .001, 0,  0,    0,   0,  0];
  upper=[inf,inf, 1,    1, inf,inf,inf, 1, inf, inf, 1, 1.9, pi/p, inf,inf];

  checklo=varn-lower;                 % If a parameter is out of limits low, the
                                      % corresponding checklo value is negative

  checkhi=upper-varn;                 % If a parameter is out of limits high, the
                                      % corresponding checkhi value is negative

  for t=1:length(varn)                % if a parameter is out of limits low, set
    if sign(checklo(t)) == -1         % it to the lower limit
      varn(t)=lower(t);
      checkall=1;
    end
  end

  for t=1:length(varn)                % if a parameter is out of limits high, set
    if sign(checkhi(t)) == -1         % it to the upper limit
      varn(t)=upper(t);
      checkall=1;
    end
  end

  if checkall == 1                    % if any parameter was changed, reset all
    Ri=varn(1);
    qs=varn(2);
    lamsi=varn(3);
    pitch=varn(4);
    p=varn(5);
    Ro=varn(6);
    qr=varn(7);
    lamri=varn(8);
    n=varn(9);
    g=varn(10);
    M=varn(11);
    Bti=varn(12);
    beta=varn(13);
    hss=varn(14);
    hsr=varn(15);
  end

end                                   % end of parameter generation

if qr==qs                             % prohibit equal number of slots on rotor and stator
  if qr < 5
    qr=qr+1;
```

```
  else
    qr=qr-1;
  end
end

if f7 == 1                  % if previous PM motor was infeasible due to
  M=1;                      % negative gap length, force current motor to PM
  f7=0;
end

if f8 == 1                  % if previous wound motor was infeasible due to
  M=0;                      % rotor slot height, force current motor to wound
  f8=0;
end

if k/1000==round(k/1000)    % running status printout
  k
end


%************************Preliminary*********************************************************

omega=(RPM*2*pi*p)/60;      % rated electrical frequency (rad/s)
Bg=Bti*(1-lamsi);           % peak flux density in gap
Tr=2*pwr/((RPM*pi/30)*n);   % torque per disk (N-m)
RR=Ro^2-Ri^2;               % common value in equations to follow

%*************************Stator*************************************************************

ss=n;                               % number of series stators=number of stages
kps=cos((pi-pi*pitch)/2);           % stator pitch factor
kbs=0.5/(qs*sin(pi/(qs*6)));        % stator breadth factor
kws=kbs*kps;                        % stator winding factor
Va=omega*RR*kws*Bg/(sqrt(2)*p);     % phase voltage (volts/turn)
S=pwr/cos(pfang);                   % apparent power (volt-amps)
Ia=S/(3*Va);                        % stator current (amp-turns)
Zb=S/(3*Ia^2);                      % base impedance (ohms/turn^2)
wss=2*pi*Ri*lamsi/(6*qs*p);         % stator slot width (m)
Ka=6*Ia/(pi*Ri*lamsi*ss);           % stator electrical loading (amp-turns/m)
Ja=Ka/(hss*packfacs);               % conductor current density (amps/m^2)

if  Ja > Jmax                       % check for excessive current density
  hss=Ka/(Jmax*packfacs);           % adjust slot height if necessary
  Ja=Jmax;                          % new conductor current density
end

if hss <= hmax*wss                  % slot height feasibility check

  Xal=8*omega*mu*hss*(Ro-Ri)/(pi*Ri*lamsi*ss);     % leakage reactance (ohms/turn^2)
  Xaao=omega*mu*kws^2*RR/(pi*g*n*p^2);             % phase reactance (ohms/turn^2)
  Xd=1.5*Xaao+Xal;                                 % synchronous reactance (ohms/turn^2)
  xd=Xd/Zb;                                        % per-unit synchronous reactance
  eaf=sqrt(1+xd^2+2*xd*sin(pfang));                % rated internal voltage (pu)
  Eaf=eaf*Va;                                      % rated internal voltage (volts/turn)
  ksi=lamsi/sqrt(1-lamsi^2);                       % slot fraction ratio
  psi=pi*pitch/(2*p);                              % 1/2 angle subtended by a turn
  Lsi=2*Ri*(((ksi*psi-1)*sqrt(ksi^2+1-2*ksi*...    % inner edge turn length (m)
  psi+ksi^2*psi^2)/ksi)+(ksi/2)*log(2*sqrt(ksi^4+ksi^2-2*ksi^3*psi+ksi^4*psi^2)+2*ksi^2*...
  psi-2*ksi)+(sqrt(ksi^2+1)/ksi)-(ksi/2)*log(2*ksi*sqrt(ksi^2+1)-2*ksi));
  lamso=Ri*lamsi/Ro;                               % slot fraction at Ro
  kso=lamso/sqrt(1-lamso^2);                       % outer slot fraction ratio
  Lso=2*Ro*(((kso*psi-1)*sqrt(kso^2+1-2*...        % outer edge turn length (m)
  kso*psi+kso^2*psi^2)/kso)+(kso/2)*log(2*sqrt(kso^4+kso^2-2*kso^3*psi+kso^4*psi^2)+2*kso^2*...
  psi-2*kso)+(sqrt(kso^2+1)/kso)-(kso/2)*log(2*kso*sqrt(kso^2+1)-2*kso));
  Lts=2*(2*(Ro-Ri)+Lsi+Lso);                       % total length of a stator turn (m)
  delRsi=Ri*ksi*psi+wss;                           % inner edge turn stack thickness (m)

  if delRsi<=Ri                                    % inner stack thickness feasibility check

    delRso=Ro*kso*psi+wss;                         % outer edge turn stack thickness (m)
    Ra=6*Lts/(condCu*pi*Ri*lamsi*hss*packfacs*ss); % stator resistance (ohm/turn^2)
    Rso=Ro+delRso;                                 % stator structural outer radius (m)
    Rsi=Ri-delRsi;                                 % stator structural inner radius (m)

    %************************Rotor*************************************************************
```

```
sr=n;                                          % number of series rotors=total rotors

if M == 0       %************* wound rotor calculations**********************************

  kr=0.5/(qr*sin(pi/(qr*6)));                  % rotor winding factor
  Ifnl=pi*Bg*n*p*g/(mu*kr);                    % no-load field current (amp-turns)
  If=Ifnl*eaf;                                 % full load current (amp-turns)
  wsr=lamri*2*pi*Ri/(2*qr*p);                  % rotor slot width (m)
  Jf=2*If/(pi*Ri*lamri*hsr*sr*packfacr);       % conductor current density (amps/m^2)

  if Jf > Jmax                                 % increase slot height if necessary
    hsr=hsr*Jf/Jmax;
    Jf=Jmax;
  end

  if hsr<=hmax*wsr                             % slot height feasibility check

    kri=lamri/sqrt(1-lamri^2);                 % inner slot fraction ratio
    psir=pi/(2*p);                             % 1/2 angle subtended by a turn (rad)
    Lri=2*Ri*(((kri*psir-1)*sqrt(kri^2+...     % inner edge turn length (m)
    1-2*kri*psir+kri^2*psir^2)/kri)+...
    (kri/2)*log(2*sqrt(kri^4+kri^2-2*kri^3*psir+kri^4*psir^2)+2*kri^2*...
    psir-2*kri)+(sqrt(kri^2+1)/kri)-(kri/2)*log(2*kri*sqrt(kri^2+1)-2*kri));
    lamro=Ri*lamri/Ro;                         % slot fraction at Ro
    kro=lamro/sqrt(1-lamro^2);                 % outer slot fraction ratio
    Lro=2*Ro*(((kro*psir-1)*sqrt(kro^2...      % outer edge turn length (m)
    +1-2*kro*psir+kro^2*psir^2)/kro)+...
    (kro/2)*log(2*sqrt(kro^4+kro^2-2*kro^3*psir+kro^4*psir^2)+2*kro^2*...
    psir-2*kro)+(sqrt(kro^2+1)/kro)-(kro/2)*log(2*kro*sqrt(kro^2+1)-2*kro));
    Ltr=2*(2*(Ro-Ri)+Lri+Lro);                 % total length of a stator turn (m)
    delRri=Ri*kri*psir+wsr;                    % inner edge turn stack thickness (m)
    delRro=Ro*kro*psir+wsr;                    % outer edge turn stack thickness (m)
    Rf=2*Ltr/(pi*Ri*lamri*hsr*condCu*...       % total field resistance (ohms/turn^2)
    sr*packfacr);
    Rro=Ro+delRro;                             % rotor structural outer radius (m)
    Rri=Ri-delRri;                             % rotor structural inner radius (m)
  end

else     %***********permanent magnet rotor calculations*********************************

  ratio1=Eaf*pi*p/(4*omega*Br*sin(p*beta/2)*RR*kws);  % ratio1=hm/(hm+2g)
  ratio2=ratio1/(1-ratio1);                           % hm=ratio2*2g
  g=(omega*mu*kws^2*RR/(Xaao*pi*n*p^2))/(ratio2+1);   % new gap length (m)
  hm=ratio2*2*g;                                      % magnet height (m)
  If=0;                                               % no field current
  Rri=Ri;                                             % no structure needed for edge turns
  Rro=Ro;
  hsr=hm;                                             % magnet mount height (m)
  delRri=0;                                           % no edge turns
  Rf=0;                                               % no field current
  wsr=inf;                                            % bypass slot height feasibility

end                                    % end of rotor calculations

if hsr<=hmax*wsr                       % slot height feasibility check
  if delRri<=Ri                        % stack thickness feasibility check
    if g >= 0.001                      % gap length feasibility check (for PM)


      %*****************************Shaft*************************************************

      sor=min([Rri,Rsi]);                                % shaft outer radius (m)
      tr=max([Tr/(2*pi*sor^2*taumax),hsr]);              % rotor disk thickness (m)
      sod=2*sor;                                         % shaft outer diameter (m)
      sid=(sod^4-(16*Tr*n*sod)/(pi*taumax))^0.25;        % shaft inner diameter (m)

      if imag(sid)==0                                    % shaft area feasibility check

        sxs=pi/4*(sod^2-sid^2);                          % shaft x-sec area (m^2)

        %*****************************Case**************************************************

        cir=max([Rso,Rro]);                                    % case inner radius (m)
        ts=max([Tr/(2*pi*cir^2*taumax),hss]);                  % stator disk thickness (m)
```

```
cid=2*cir;                                              % case inner diameter (m)
clear cod1
cod1=roots([1,0,0,-16*Tr*n/(taumax*pi),-cid^4]);        % max stress criteria

for y=1:length(cod1)                                    % select smallest root > cid
  if imag(cod1(y)) ~= 0
    cod1(y)=1e99;
  end
  if cod1(y) < cid
    cod1(y)=1e99;
  end
end

cod=min(cod1);                                  % case outer diameter (m)

if cod < codmax                                 % machine diameter feasibility check

  %*************************Weight and Volume************************************

  tb=((Ro+Ri)/p)*(Bg/Bsat);                     % back iron depth (m)
  volbi=2*pi*RR*tb;                             % back iron volume (m^3)
  wb=volbi*rhoes;                               % back iron weight (kg)
  volsi=pi*RR*(1-lamsi)*2*hss;                  % stator iron volume (m^3)
  volss=pi*(Rso^2-Rsi^2)*ts;                    % stator steel volume (m^3)
  volsw=Lts*hss*pi*Ri*lamsi;                    % stator copper volume (m^3)
  volsins=volsw*(1-packfacs)/packfacs;          % stator insulation volume (m^3)
  wstat=volsw*rhoCu+volsins*rhoins+volss*rhoss+volsi*rhoes;  % stator weight (kg)

  if M == 0                                     % wound rotor volumes

    volri=pi*RR*(1-lamri)*2*hsr;                % rotor iron volume (m^3)
    volrw=Ltr*hsr*pi*Ri*lamri;                  % rotor copper volume (m^3)
    volrins=volrw*(1-packfacr)/packfacr;        % rotor insulation volume (m^3)
    volPM=0;                                    % rotor magnet volume (m^3)

  else                                          % permanent magnet rotor volumes

    volri=RR*(pi/p-beta)*2*hm*2*p;              % rotor iron volume (m^3)
    volrw=0;                                    % rotor copper volume (m^3)
    volrins=0;                                  % rotor insulation volume (m^3)
    volPM=pi*RR*hm-volri;                       % rotor magnet volume (m^3)

  end

  volrs=pi*(Rro^2-sor^2)*tr;                    % rotor steel volume (m^3)
  wrot=volrw*rhoCu+volrins*rhoins+...           % rotor weight (kg)
  volrs*rhoss+volri*rhoes+volPM*rhoPM;
  sl=n*(2*hsr+tr+2*hss+ts+2*g)+2*tb;            % stack length (m)

  if sl < slmax                         % stack length feasibility check

    vols=sl*sxs;                        % shaft volume (m^3)
    ws=vols*rhoss;                      % shaft weight (kg)

    %*******************Shaft and Case Bending and Runout************************

    sid1=sid;                           % temporary shaft inner diameter
    wdist=(n*wrot+ws)/sl;               % weight per unit length on shaft (kg/m)
    Izz=(pi/32)*(sod^4-sid1^4);         % shaft second moment of area (m^4)
    Lmax=2*sqrt(4*taumax*Izz/(sod*wdist));    % max length between supports (m)

    while floor(sl/Lmax) > 0;                   % reduce sid1 if stress > max

      sid1=sid1-0.005;                          % increase shaft thicknes by 1/2 cm
      sxs=pi/4*(sod^2-sid1^2);                  % new shaft cross sectional area
      vols=sl*sxs;                              % new shaft volume
      ws=vols*rhoss;                            % new shaft weight
      wdist=(n*wrot+ws)/sl;                     % new weight per unit length
      Izz=(pi/32)*(sod^4-sid1^4);               % new second moment of area
      Lmax=2*sqrt(4*taumax*Izz/(sod*wdist));    % new max length

     if sid1 <= 0                               % if sid1 goes to zero, exit & flag
        sid1=0;
        Lmax=1e99;
      end
```

```
end                                          % end of while floor(sl/Lmax) > 0

if Lmax ~= 1e99                              % bypass if infeasible in bending

  runout=0.125*wdist*(Lmax/2)^4/(Es*Izz); % shaft runout (%)
  sro=runout/Lmax;                           % compare to max allowed

  while sro > sromax                         % decrease sid1 if necessary

    sid1=sid1-0.005;                         % increase shaft thickness by 1/2 cm
    sxs=pi/4*(sod^2-sid1^2);                 % new shaft cross sectional area
    vols=sl*sxs;                             % new shaft volume
    ws=vols*rhoss;                           % new shaft weight
    wdist=(n*wrot+ws)/sl;                    % new weight per unit length
    Izz=(pi/32)*(sod^4-sid1^4);                    % new second moment of area
    runout=0.125*wdist*(Lmax/2)^4/(Es*Izz);        % check shaft runout
    sro=runout/Lmax;                               % compare to max allowed

  end                                        % end of while sro > max

  if sid1 ~= sid                             % if sid has been modified
    cod=cod*(sid/sid1);                      % increase case thickness
    sid=sid1;
  end

  volc=pi/4*(cod^2-cid^2)*sl;                % case volume (m^3)
  wc=volc*rhoss;                             % case weight (kg)
  volm=pi/4*cod^2*sl;                        % machine volume (m^3)
  wm=n*(wrot+wstat)+wc+wb+ws;                % machine weight (kg)

  if sl/cod <= 1.0                           % length to diameter function
    l_d=1;
  else
    l_d=-(1/3)*(sl/cod)+(4/3);
  end

  %************************Rated Losses*****************************************

  Culs=3*Ra*Ia^2;                            % total stator copper loss
  cl=(8.86*(Bg/sqrt(2))^1.88*(omega/...      % total hysteresis loss
  377)^1.53)*((volbi+volri+volsi)*rhoes+volPM*rhoPM);
  Culf=If^2*Rf;                              % total field copper loss
  totl=Culs+cl+Culf;                         % total losses

  nu=S/(S+totl);                             % rated efficiency
  hdens=totl/volm;                           % rated heat density

  %************************Losses at Average Power*******************************

  avgomega=omega*(avgRPM/RPM);     % electrical frequency at avg power (rad/s)
  avgpwr=pwr*(pctpwr/100);         % average power (Watts)
  avgS=avgpwr/cos(pfang);          % avg apparent power (volt-amps)
  avgXd=(avgomega/omega)*Xd;       % sync reactance at avg power(ohms/turn^2)

  if M==0                          % efficiency calcs @ avg power, wound rotor

    Ialow=avgS/(3*Va);                       % avg stator current at Va=1 pu
    avgIaw=[1e-6:(Ia-Ialow)/100:Ia];         % avg Ia vector (amp-turns)
    avgVaw=avgS./(3*avgIaw);                 % avg Va vector (volts/turn)
    avgXdIaw=avgXd*avgIaw;                   % avg reactance vector (volts/turn)
    avgEafw=sqrt(avgVaw.^2+avgXdIaw...       % avg Eaf vector (volts/turn)
    .^2-2.*avgVaw.*avgXdIaw*cos(pfang+pi/2));
    avgIfw=Ifnl*avgEafw/Eaf;                 % avg field current (amp-turns)
    avgCulsw=3*Ra*avgIaw.^2;                 % avg stator copper loss (Watts)
    avgCulfw=avgIfw.^2*Rf;                   % avg field copper loss (Watts)
    avgclw=(8.86*(Bg*avgomega/...            % avg core loss (Watts)
    (omega*sqrt(2)))^1.88*(avgomega/377)^1.53)*(volbi+volri+volsi)*rhoes;
    avgtotlw=avgCulsw+avgCulfw+avgclw;       % avg total losses (Watts)
    avgnuw=avgS./(avgS+avgtotlw);            % avg efficiency

    nuavg=max(avgnuw);                       % max efficiency at avg power

  else                             % efficiency calcs @ avg power, PM rotor
```

```
  avgEafp=(hm/(hm+2*g))*...                          % avg internal voltage
  4*avgomega*Br*sin(p*beta/2)*RR*kws/(pi*p);
  avg_Iap=roots([avgXd^2,0,-avgEafp^2...             % solve 4th order for avgIap
  -(2*avgS*avgXd*cos(pfang+pi/2)/3),0,avgS^2/9]);
  avgIap=min(abs(avg_Iap));                          % minimum positive root
  avgclp=(8.86*(Bg*avgomega/...                      % avg core loss (Watts)
  (omega*sqrt(2)))^1.88*(avgomega/377)^1.53)*...
  ((volbi+volri+volsi)*rhoes+volPM*rhoPM);
  avgCulsp=3*Ra*avgIap^2;                            % avg stator copper loss
  avgtotlp=avgCulsp+avgclp;                          % avg total losses

 nuavg=avgS/(avgS+avgtotlp);                         % avg efficiency

end                                                % end of off-rated efficiency calcs

%*****************************Cost*****************************************

Cucost=n*(volsw+volrw)*CCu;                                % copper cost
inscost=n*(volsins+volrins)*Cins;                          % insulation cost
ssteelcost=(n*(volss+volrs)+volc+vols)*Cssteel;            % steel cost
esteelcost=(n*(volsi+volri)+volbi)*Cesteel;                % iron cost
PMcost=volPM*CPM;                                          % magnet cost
matcost=Cucost+inscost+ssteelcost+esteelcost+PMcost;       % materials cost
rt=1;                                                      % rotor type factor
if M==0
  rt=confacw;
end
constcost=(0.8*n+0.2)*daybase*labday*rt;                   % construction cost
acqcost=(1+1/pmarg)*(matcost+constcost);                   % acquisition cost

fuelcost=(wtfuel/nuavg)*Cfuel;                             % lifetime fuel cost

totcost=acqcost+fuelcost*disfac;                           % total cost

%*************************************************EVALUATION*****************************************
%*****************************************************************************************************

f6=f6+1;                                  % f6 = 1 for first feasible motor
attrib=[Ri,qs,lamsi,pitch,p,Ro,...        % vector of parameters and attributes
qr,lamri,n,g,M,hss,hsr,sl,...
cod,nu,volm,wm,hdens,l_d,eaf,totcost,Bti,beta]';

if f6 > 1          % skip if k is first feasible motor
  clear temp       % temporary holding matrix
  f1=0;            % column index for temp
  f2=0;            % flag (set to 1 if k is dominated by any
                   % motor on frontier)

  [A,B]=size(frontier);
  runsize(f6)=B;  % track frontier size for plotting
  f8=0;            % f8=1 for first frontier motor dominated by k
  for m=1:B        % This loop checks k against each motor on
                   % the current frontier.  If a motor on the
                   % frontier is not dominated by k, that motor
                   % is placed in temp to be retained.  Also,
                   % if k itself is not dominated by any motor
                   % on the frontier, k is placed in temp after
                   % all motors have been checked. The frontier
                   % is then set equal to temp and the program
                   % generates the next motor.  If k is
                   % dominated by any motor, the process is
                   % halted and the frontier is preserved.

    if f2 == 0     % terminate if k has been dominated
      f3=0;        % dominance sum: 6=k dominant  0=k dominated

      % Note:  1% margins are required for dominance.
      % The constants 1.01 and 0.99 implement this.

      if nu >= 1.01*frontier(16,m)              % k dominant in efficiency?
        f3=f3+1;
      end
```

```
                if volm <= 0.99*frontier(17,m)          % k dominant in volume?
                  f3=f3+1;
                end

                if wm <= 0.99*frontier(18,m)            % k dominant in weight?
                  f3=f3+1;
                end

                if hdens <= 0.99*frontier(19,m)         % k dominant in hdens?
                  f3=f3+1;
                end

                if l_d >= 1.01*frontier(20,m)           % k dominant in l_d ratio?
                  f3=f3+1;
                end

                if totcost <= 0.99*frontier(22,m)       % k dominant in cost?
                  f3=f3+1;
                end

                if f3 < 6                               % if k is not dominant
                  f1=f1+1;                              % increment temp index
                  temp(:,f1)=frontier(:,m);             % add frontier motor
                end                                     % to temp

                if f3 == 0                  % if k is dominated by this motor
                  f2=1;                     % set flag to discontinue comparisons
                  clear temp                % preserve current frontier
                  temp=frontier;
                end

                if f3 == 6                  % if k dominates, use Gaussian for k+1
                  f4=1;
                  f5=k;
                  f8=f8+1;                  % counter for number of motors dominated by k
                  if f8==1                  % retain hit motor's parameters
                    Rih=Ri;
                    qsh=qs;
                    lamsih=lamsi;
                    pitchh=pitch;
                    ph=p;
                    Roh=Ro;
                    qrh=qr;
                    lamrih=lamri;
                    nh=n;
                    gh=g;
                    Mh=M;
                    Btih=Bti;
                    betah=beta;
                    hssh=hss;
                    hsrh=hsr;
                  end
                end

              end                   % end of if f2=1 (has k been dominated)

            end                     % k has either been compared to all motors
                                    % in frontier or has been dominated.
            if f2 == 0              % if k was not dominated
              temp(:,f1+1)=attrib; % add k to temp
            end
            clear frontier          % redefine frontier
            frontier=temp;

          else                      % frontier is initiated by first feasible motor
            frontier(:,1)=attrib;
          end               % end of check for 1st feasible motor
        end                 % end of if Lmax ~= 1e99
      end                   % end of stack length limit check
    end                     % end of machine diameter limit check
  end                       % end of imag sid
else                        % PM gap length feasibility:  force next to PM
  f7=1;
end          % end of gap length feasibility check
end          % end of delRri<=Ri feasibility check
```

```
      else              % wound slot height feasibility:  force next to wound
        f8=1;
      end               % end of hsr feasibility check
    end                 % end of delRsi<=Ri feasibility check
  end                   % end of hss feasibility check
end                     % end of main loop

clockend=clock;
time=[clockstart(4),clockstart(5);clockend(4),clockend(5)]  % matrix of start and end times

ans2=input('Overwrite previous frontier?     ','s');        % this appends these results
                                                            % to the previous database,
if ans2=='y'                                                % stored in this directory as
                                                            % base.mat
  if ans1=='y'
    its=its+total;                          % total iterations performed for this database
  else
    its=total;
  end
  save base frontier f4 f6 f7 runsize its;
end
```

Appendix C: Parameter Frontier Distributions

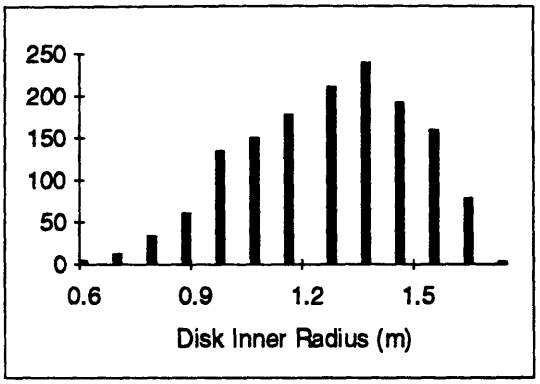

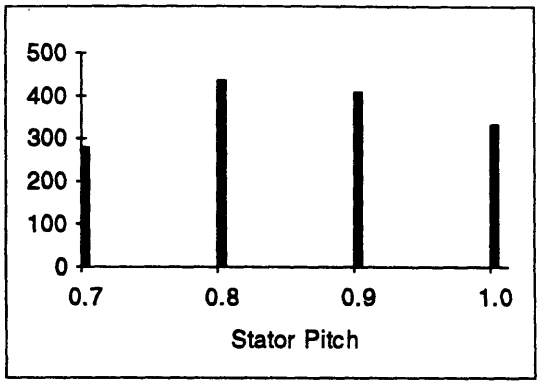

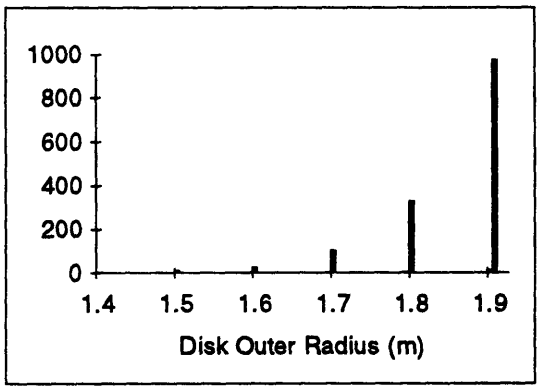

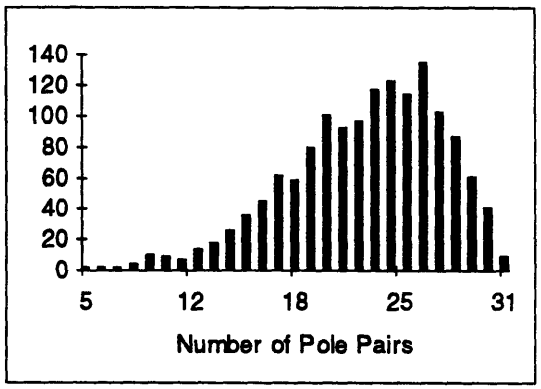

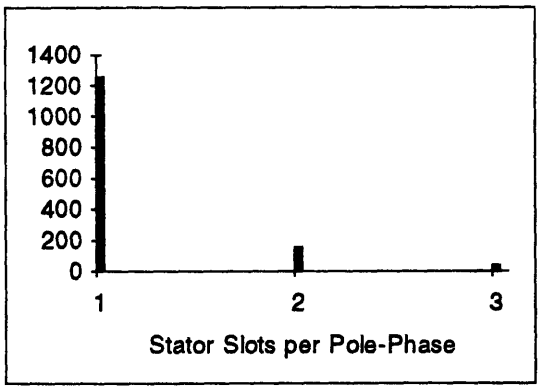

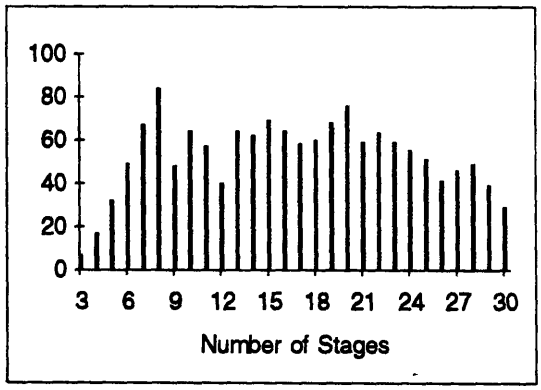

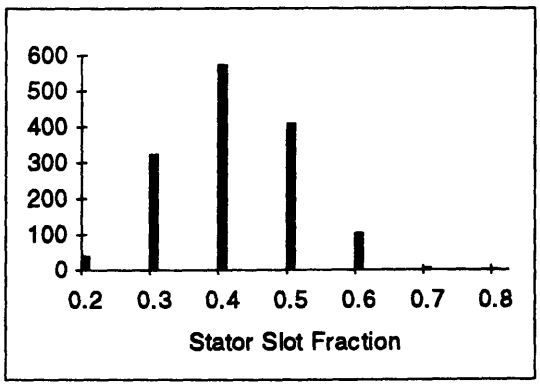

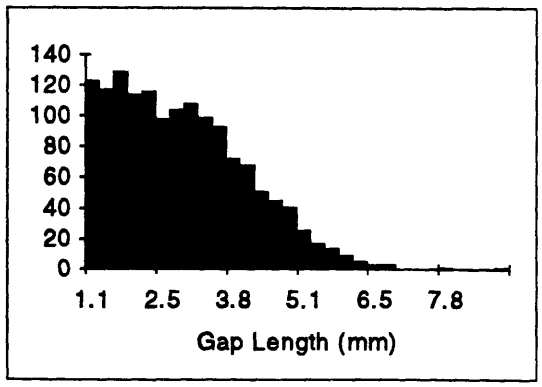

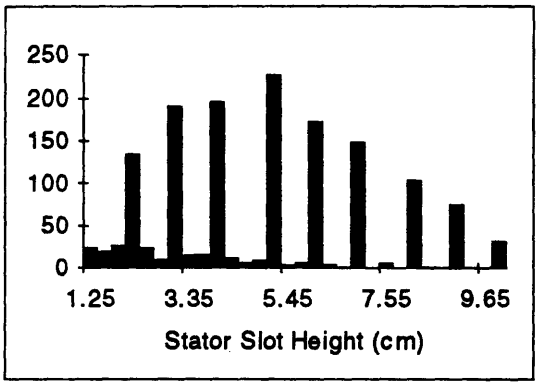
250
200
150
100
50
0
1.25
3.35
5.45
7.55
9.65
Stator Slot Height (cm)

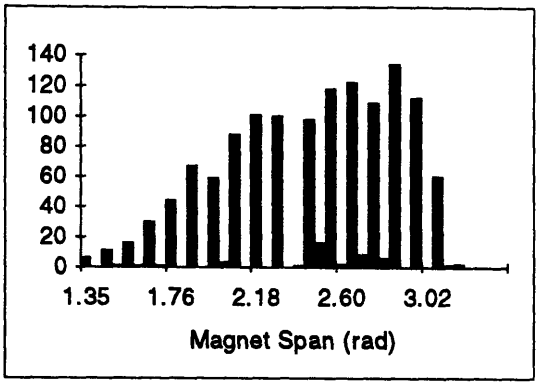
140
120
100
80
60
40
20
0
1.35
1.76
2.18
2.60
3.02
Magnet Span (rad)

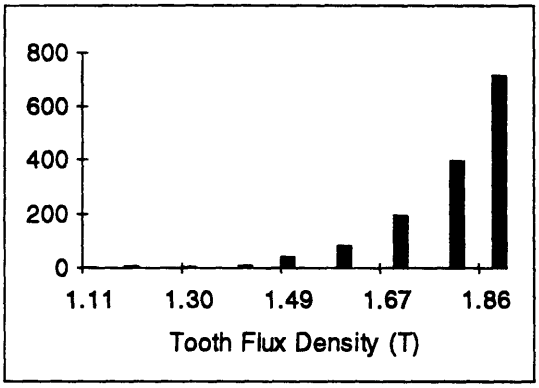
800
600
400
200
0
1.11
1.30
1.49
1.67
1.86
Tooth Flux Density (T)

Appendix D: Attribute Frontier Distributions

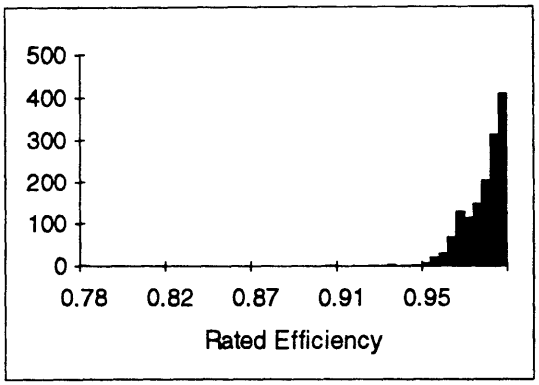

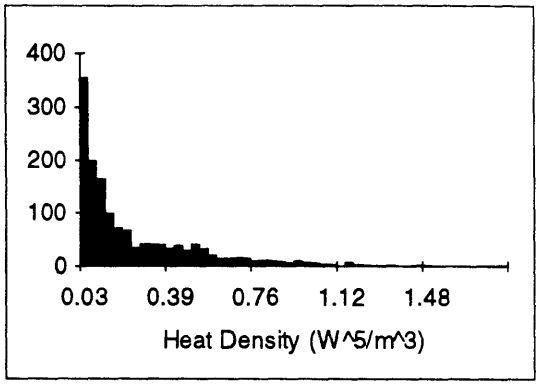

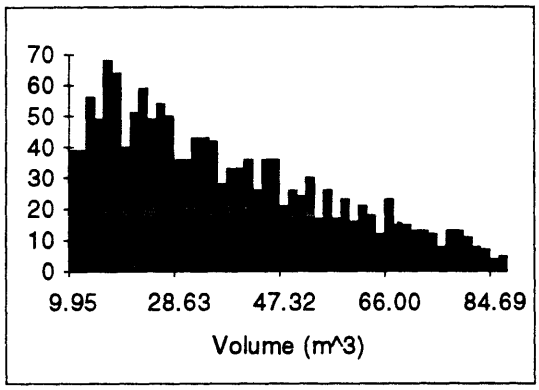

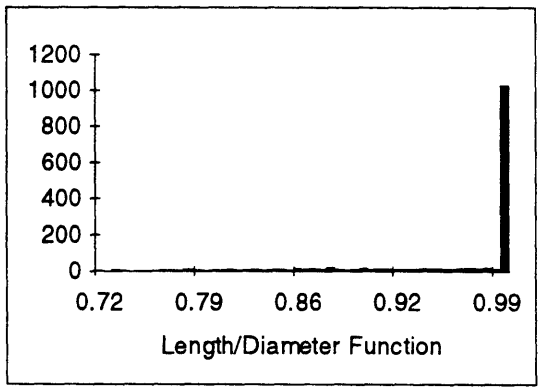

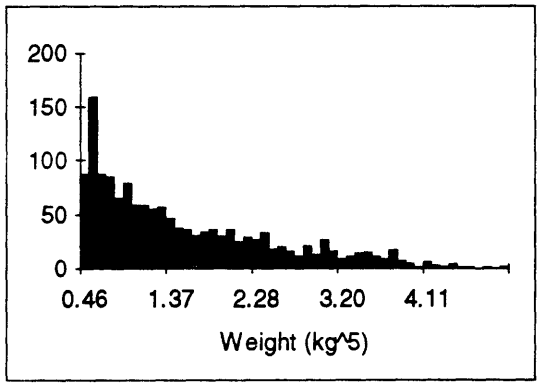

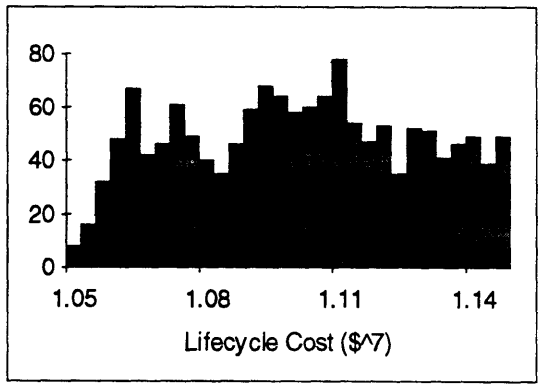

References

[1] Timothy J. McCoy, "Thermosyphon-Cooled Axial Gap Electric Motors," Ph.D. Thesis, Massachusetts Institute of Technology, May 1994.

[2] J. A. Moses, J. L. Kirtley Jr., J. H. Lang, R. D. Tabors, and F. De Cuadra, "A Computer-Based Design Assistant for Induction Motors," IEEE Industry Applications Society Conference, September 30, 1991, Dearborne, Michigan.

[3] Ujjwal Sinha, "A Design Assistant for Induction Motors," MS Thesis, Massachusetts Institute of Technology, August 1993.

[4] LT Cliff Whitcomb, "PEBB Systems Engineering," presentation given at the Office of Naval Research Industrial Workshop, June 1995.

[5] Stephen H. Crandall, Norman C. Dahl, and Thomas J. Lardner, *An Introduction to the Mechanics of Solids*, 2nd ed., McGraw-Hill, 1978.

[6] Koichi Masubuchi, "Steels," Class Notes Ch. 8 for Course 13.15J *Materials*, Massachusetts Institute of Technology, February 1994.

[7] A. E. Fitzgerald, Charles Kingsley Jr., and Stephen D. Umans, *Electric Machinery*, 5th ed., McGraw-Hill, 1990.

[8] James L. Kirtley Jr., "Winding Inductances," Class Notes #5 for Course 6.685 *Electric Machines*, Massachusetts Institute of Technology, February 1995.

[9] James L. Kirtley Jr., "Squirrel Cage Machine Model," Class Notes #8 for Course 6.685 *Electric Machines*, Massachusetts Institute of Technology, February 1995.

[10] James L. Kirtley Jr., "Air-Core Armature Shape: A Comparison of Helical and Straight- With-End-Turns Windings," presented at The International Conference on Evolution and Modern Aspects of Synchronous Machines, Zurich, August 1991.

[11] George F. Simmons, *Calculus with Analytic Geometry*, McGraw-Hill, 1985

[12] William H. Beyer, *Standard Mathematical Tables*, 26th ed., CRC Press 1981.

[13] E. P. Popov, *Mechanics of Materials*, Prentice-Hall, 1978.

[14] James L. Kirtley Jr., "Iron and Magnetic Materials," Class Notes #10 for Course 6.685 *Electric Machines*, Massachusetts Institute of Technology, March 1995.

[15] Interviews with Dr. Tom Keim, Sc.D., of Kaman Electromagnetics Corporation, February-March 1996.

[16] Interviews with James L. Kirtley Jr., Ph.D., Professor of Electrical Engineering, Massachusetts Institute of Technology, January-April 1996.

[17] E. Paul De Garmo, W. G. Sullivan and J. A. Bontadelli, *Engineering Economy*, 9th ed., Macmillan Publishing, New York, 1993.

[18] H. C. Schlappi, "Energy Saving Propulsion System," *Naval Engineers Journal*, April 1982.

[19] Alvin W. Drake, *Fundamentals of Applied Probability Theory*, McGraw-Hill, 1988.

[20] Donald L. Harnett, *Statistical Methods*, 3rd ed., Addison-Wesley, 1982.

[21] Francis R. Colberg, "Damage Analysis of Internal Faults in Flux Concentrating Permanent Magnet Motors," Naval Engineer/SM Thesis, Massachusetts Institute of Technology, May 1994.